Chapter 14 in the book:
P.A. Kralchevsky and K. Nagayama, "Particles at Fluid Interfaces and Membranes," Elsevier, Amsterdam, 2001; pp. 591-633.

CHAPTER 14

EFFECT OF OIL DROPS AND PARTICULATES ON THE STABILITY OF FOAMS

In some cases the foaminess is desirable, while in other cases it is not wanted. The attachment of μm-sized oil droplets and/or solid particles to fluid interfaces has a foam-destabilizing effect, which can be used as a tool for control of foam stability. In this aspect the knowledge about the mechanism of antifoaming action could be very helpful. Direct observations show that when the foam decay is slow, the antifoam particles are expelled from the foam films into the Plateau borders, where the particles may enter the air-water interface and destroy the neighboring foam cell(s). In contrast, when the particles exhibit a fast antifoaming action, they are observed to directly break the foam films, which thin much faster than the Plateau borders.

Three different mechanisms of antifoaming action have been established: spreading mechanism, bridging-dewetting and bridging-stretching mechanism. All of them involve as a necessary step the entering of an antifoam particle at the air-water interface, which is equivalent to rupture of the asymmetric particle-water-air film. Criteria for spontaneous occurrence of entering, spreading and bridging have been proposed. The experiment shows that the key determinant for antifoaming action is the stability of the asymmetric particle-water-air film. Repulsive interactions in this film may create a high barrier to drop entry. The major thermodynamic factors, which stabilize the asymmetric film, are the disjoining-pressure barriers due to the double layer repulsion, steric polymer-chain interaction, and oscillatory structural forces. In addition, there are kinetic stabilizing factors, such as the surface elasticity and viscosity, which damp the instabilities in the liquid films. On the other hand, a destabilizing factor can be any attractive force operative in the liquid films, as well as any factor suppressing the effect of the aforementioned stabilizing factors. Solid particulates of irregular shape, adsorbed at the oil-water interface, have a "piercing effect" on the asymmetric oil-water-air films. The evaporation from a foam can also help for overcoming the disjoining-pressure barrier(s). The accumulated knowledge about the mechanisms of foam destruction enables one to give definite predictions and prescriptions concerning the foam stability after a careful examination of the factors operative in each specific case.

14.1. FOAM-BREAKING ACTION OF MICROSCOPIC PARTICLES

14.1.1. CONTROL OF FOAM STABILITY; ANTIFOAMING VS. DEFOAMING

Foams have many applications in industry and in every-day life. In some cases the formation of foams is desirable (under a certain control); such are the applications in personal-care and house-hold detergency, in fire-fighting, ore flotation, foods and drinks. On the other hand, in many cases the spontaneous formation of foams is not wanted insofar as it hampers the efficient operation of industrial processes such as paper pulp processing, paper making, polymer, sugar and food processing, textile dyeing and scouring, wastewater treatment, fermentation in pharmaceutical, food and chemical technologies, phosphoric acid production, gas-oil and distillation separation processes in petroleum industry [1-6].

It has been established that microscopic oil droplets or solid particles [7-11], and their combination [4-6, 12-16], may exhibit a foam-destructive effect. For example, small oil droplets dispersed in shampoos provide hair conditioning; special surfactant compositions have been invented to protect the foams from the destructive action of the droplets [17]. In other cases, very active antifoams are intentionally added to suppress the development of unwanted foamability during industrial processes [18]. In both cases one could achieve the desired effect utilizing the knowledge about the foam-breaking action of microscopic oil drops and particulates.

Often the investigators distinguish between defoaming and antifoaming as two different methods for foam destabilization [5, 6]. In *defoaming* first the foam is formed and then the foam-breaking agent is added onto the foam. In *antifoaming* first the foam-inhibiting agent (antifoam) is dispersed in the foaming solution, and then foam is produced, which is less stable and less voluminous because of the action of the agent.

Defoamers added on the top of an existing foam (Fig. 14.1a) begin to break the foam films one after another. Water-insoluble alcohols (like octanol) are good defoamers but ineffective as antifoams [6,19]. A possible mechanism of action of oily defoamer droplets is that they spread on one of the two surfaces of the foam films thus creating asymmetric (water-oil) films, which exhibit a kinetic instability during the process of oil spreading. The mechanism of defoaming action of hydrophobic *solid* particles could be attributed to the fact that they quickly adsorb

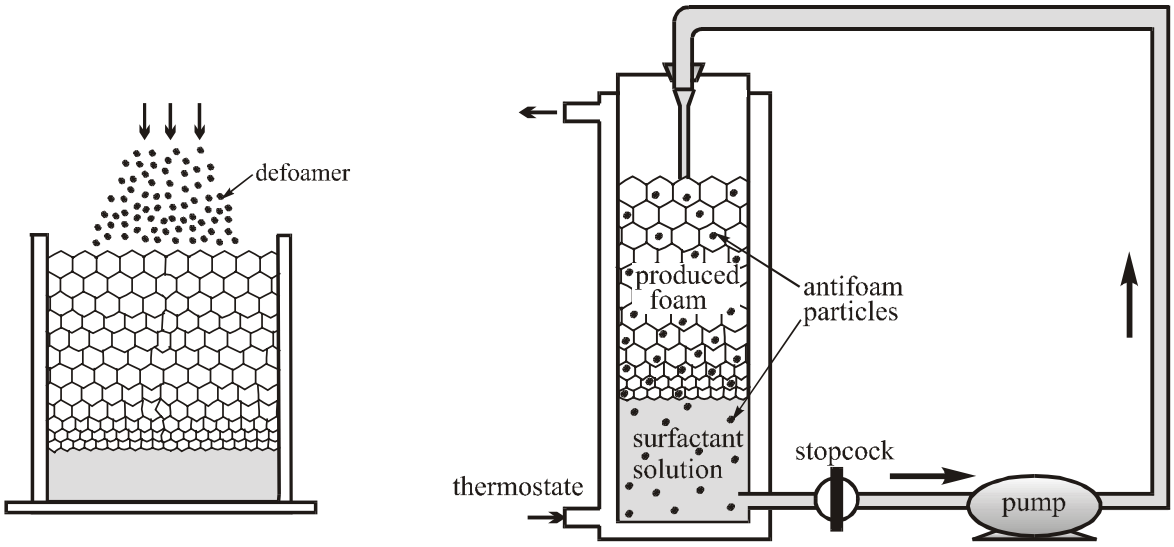

Fig. 14.1. (a) *Defoamer* particles are added on the top of existing foam; they break the foam films one after another. (b) *Antifoam* particles are contained in the solution before the production of foam; they are drawn into the newly created foam, which can be obtained by circulation of solution, as depicted in the figure.

surfactant molecules from the water-air interfaces in the foam thus creating destructive local chemical shocks [5, 12]. Note that the defoamer particles approach the air-water interfaces from the side of the *air* phase.

Antifoam particles, initially contained in the solution (Fig. 14.1b), approach the air-water interfaces from the side of the *water* phase. Sometimes (as in the case of shampoos) their antifoaming action is an undesirable side effect; in other cases they are added on purpose. As already mentioned, three types of particles are known to exhibit antifoaming action [5, 6]:

(i) *nonpolar oils*, which can be silicone or organic, including nonionic surfactants above their cloud point and some fatty esters;

(ii) *hydrophobic solid particles*: hydrophobized silica, microcrystalline waxes, hydrophobic polymers, etc.; particles of irregular shape might have a strong antifoaming effect;

(iii) *mixtures of nonpolar oils and hydrophobic solid particles*: in combination their foam-breaking activity increases synergistically.

As mentioned above, in the present chapter our attention is focused on the mechanism of action

of fluid and solid particles, which exhibit antifoaming performance. The latter is related to the attachment of the particles to the surfaces of the foam films and/or the adjacent Plateau borders.

14.1.2. STUDIES WITH SEPARATE FOAM FILMS

Before considering the mechanisms of antifoaming action (Section 14.2), it is helpful to present some research methods and illustrative examples.

The process of foam generation involves the formation of liquid films and the drainage of liquid out of the films, along the Plateau borders [20,21]. The antifoaming particles migrate throughout the foam driven by the flow of water. Model experiments with separate films can provide information about the stages of film thinning and particle migration [22,23]. A useful tool for investigating separate *horizontal* liquid films is the Scheludko cell [24,25], whose construction is shown in Fig. 14.2. Within such a cell one could form either foam films (gas-water-gas), emulsion films (oil-water-oil), or asymmetric (oil-water-gas) films. It allows one to measure the lifetime of the separate foam films, the variation of film thickness, contact angle and capillary pressure during the process of film drainage. Higher capillary pressures can be achieved with the experimental cell of Mysels [26], in which the ejection of liquid is realized by means of a porous glass plate. In particular, the film thickness can be measured by means of the micro-interferometric method, see e.g. Refs. [27-30].

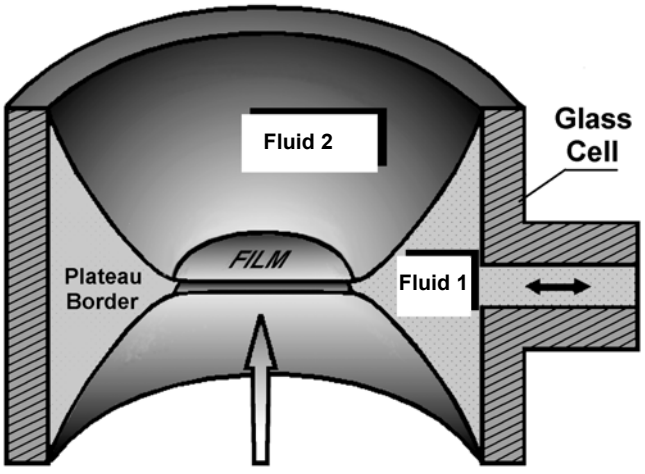

Fig. 14.2. Sketch of the experimental cell constructed by Scheludko and Exerowa [24,25]. First the cylindrical glass cell is filled with Fluid 1; next it is immersed in Fluid 2; then a portion of Fluid 1 is sucked out from the cell through the orifice in the glass wall. Thus in the central part of the cell a liquid film is formed, which is encircled with a Plateau border.

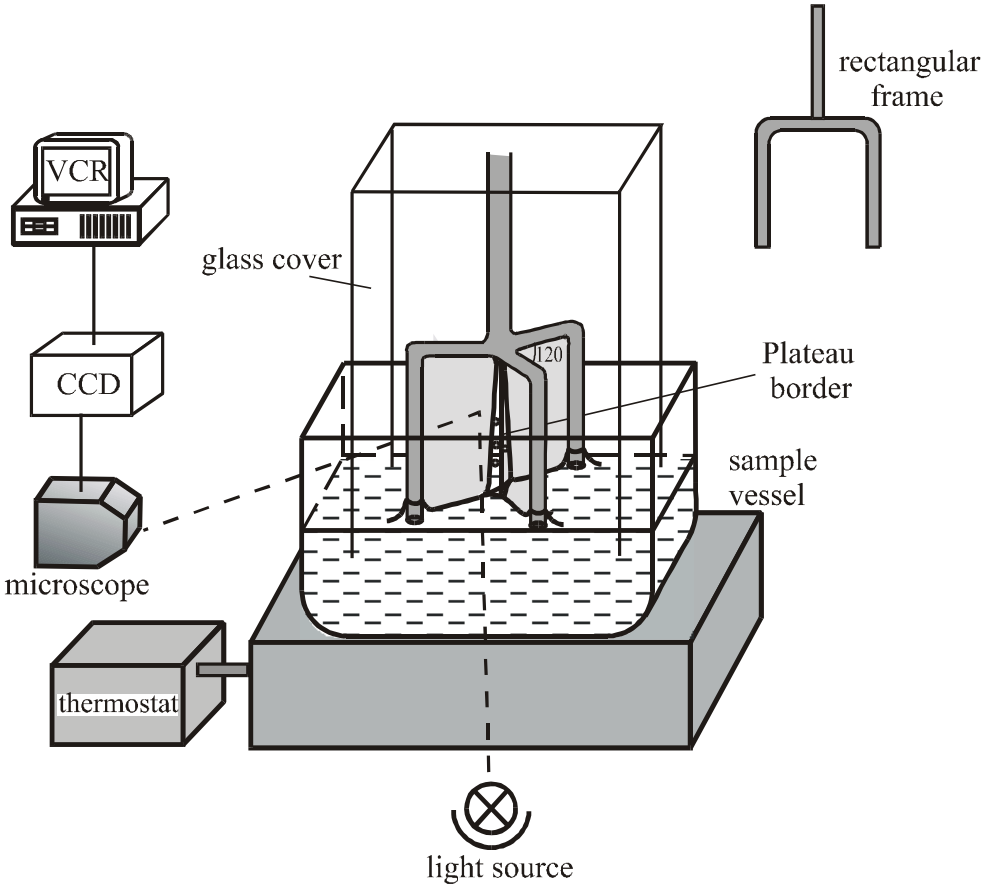

Fig. 14.3. Sketch of an experimental cell for measurements with vertical films formed by pulling up a glass frame out of the surfactant solution. One can use a simple rectangular frame (up-right) or the "three-leg" frame constructed by Koczo and Racz [31]. The formed vertical films are observed with a horizontal microscope connected to CCD camera and video recorder.

The area of the foam films has a significant effect on their stability. The films formed in the Scheludko cell are relatively small (less than a millimeter in diameter), while the films in the real foams can be larger. Moreover, the films in real foams are in contact with Plateau borders of triangular cross section, whose area decreases with time due to the water drainage out of the foam. The oil droplets can be trapped in the narrowing Plateau borders with subsequent drop entry at the surface and destruction of the neighboring foam films. The latter processes cannot be modeled in the Scheludko cell, where the Plateau border is not similar to that in the real foams. Vertical foam films of size several centimeters can be formed by pulling pull up a frame out of the surfactant solution [31,17]. A special frame with three “legs” was proposed in Ref. 31; it allows one to form simultaneously 3 vertical films, subtending angles of 120° with each other and forming a vertical Plateau border, see Fig. 14.3. This configuration allows one

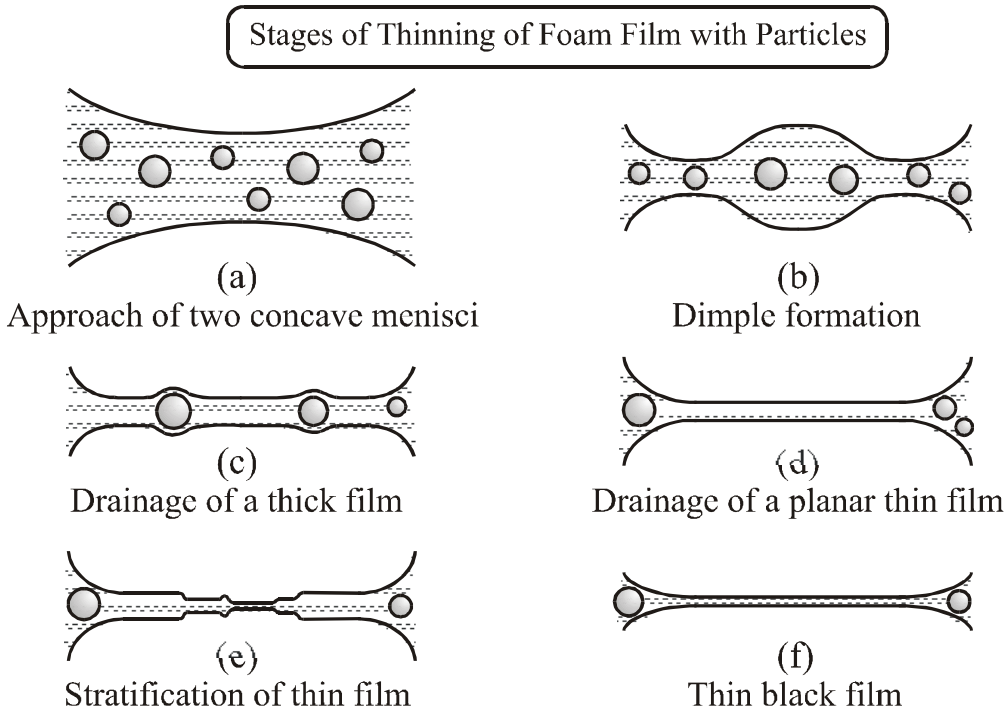

Fig. 14.4. Schematic presentation of the main evolution stages of a foam film, which is formed in a Scheludko cell from surfactant solution containing μm-sized oil drops; after Refs. [17, 18].

to study the behavior of large foam films and the effect of oil drops on the stability of Plateau borders. The "three-leg" frame enables one to obtain information about the rate of film drainage, film lifetime, period of time needed for formation of black film, critical thickness of rupture (or equilibrium film thickness), etc. [17].

Aronson [32] observed that during the process of film thinning the antifoam particles quickly move out of the foam films and enter the Plateau borders, where they are carried along by the flow of the outgoing water. This was confirmed in the experiments of Wasan et al. [23] and Koczo et al. [33] with separate foam films, both horizontal and vertical.

Figure 14.4 illustrates the consecutive stages of thinning of a horizontal liquid film initially containing oil droplets, as observed by Denkov et al. [17,18] in experiments with Scheludko cell. In the beginning a thick liquid layer is formed between the two approaching concave menisci (Fig. 14.4a). Next, due to the hydrodynamic interaction between the two liquid surfaces a thicker lens-shaped zone appears in the middle of the film, which is usually termed “dimple formation” [34], see Fig. 14.4b. Particles are observed both in the initial thick layer

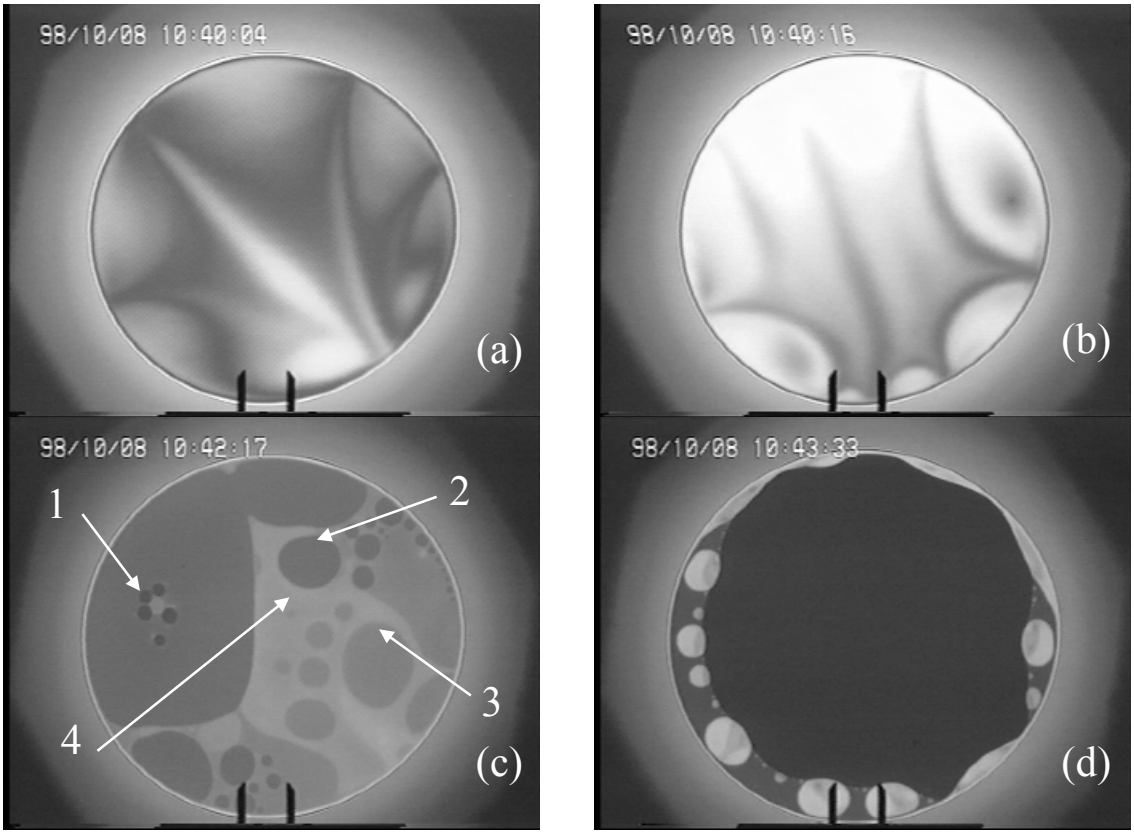

Fig. 14.5. Consecutive video-frames from Ref. [17] taken in light reflected from a thinning foam film, which is produced in a Scheludko cell from 0.1 M solution of the anionic surfactant sodium dodecyl-trioxyethylene-sulfate (SDP3S); additional non-amphiphilic electrolyte of ionic strength 0.066 M and 0.1 wt% silicone-oil droplets of average size 5 μm are also present. (a) Channel-like pattern formed after the outflow of the dimple; average film thickness $h \approx$ 550 nm. (b) Pattern at thickness 100 nm: small emulsion drops are seen (down-left and up-right). (c) Appearance of stratification spots: four levels of step-wise thinning are seen; the number of micelle layers is denoted. (d) After the last step-wise transition, a black film is formed, which does not contain surfactant micelles. The scaling bar corresponds to 100 μm.

and in the dimple. The latter is a unstable formation which soon disappears leaving some transient channel-like patterns (Fig. 14.5a). After that, an almost plane parallel film is formed, which initially may contain some oil drops (Figs. 14.4c and 14.5b), but they are soon expelled into the adjacent Plateau border driven by the water outflow from the thinning film (Fig. 14.4d). If the volume fraction of the surfactant micelles in the solution is high enough, one can observe step-wise thinning (stratification of the film), see Figs. 14.4e and 14.5c,d. Each of the steps (which appear as spots of different darkness) represents a liquid film containing a

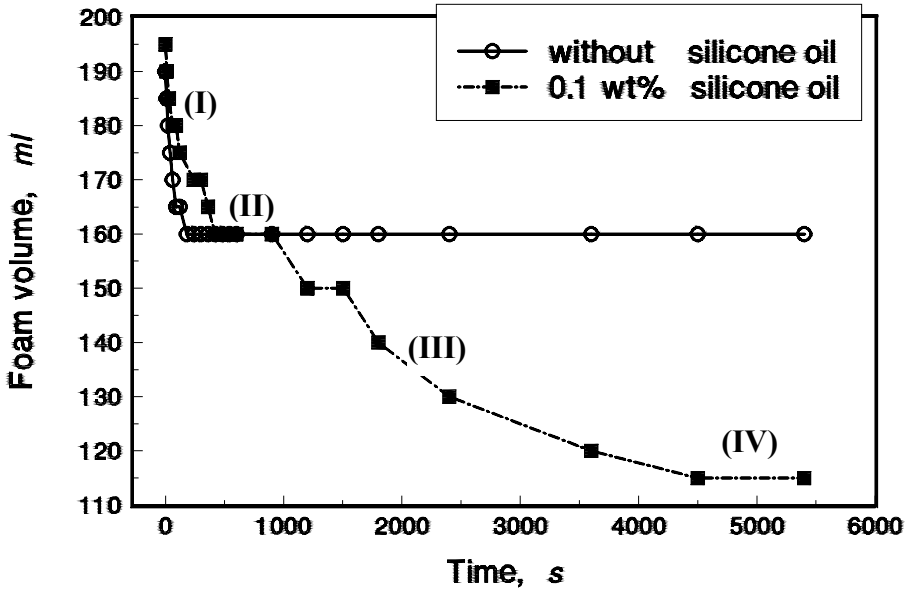

Fig. 14.6. Effect of oil drops on the decay of a foam column: experimental data from Ref. [17] for the foam volume vs. time. The foam has been produced in a setup like that in Fig. 14.1b from solution containing 0.1 M blend of 80 % anionic surfactant, SDP3S, and 20 % amphoteric surfactant, lauryl-amide-propyl-betaine. *Stage I*: drainage of water out of the foam and formation of foam cells; *Stage II*: narrowing of the Plateau borders at constant foam volume; *Stage III*: decrease of the foam volume due to destruction of foam cells by oil drops located in the Plateau borders; *Stage IV*: the antifoaming action of the oil drops is completed and the foam volume remains constant. Stages III and IV appear on the curve which corresponds to solution containing 0.1wt% added silicone-oil emulsion of average drop-size 15 μm.

given number of micelle layers: from 4 down to 0 in Figs. 14.5c,d. Finally, a thin black film is formed, which contains neither antifoam particles nor micelles (Figs. 14.4f and 14.5d).

Based on similar observations Koczo et al. [33] suggested that the rupture of foam cells does not happen by direct breaking of the foam films by the particles (at the stage depicted in Fig. 14.4c), instead, rupturing occurs when the particles become trapped in the thinning Plateau borders. This is typical for systems, in which the particles cause a *slow* foam decay (from 5 min to hours).

Figure 14.6 gives a typical example for such a system [17]: the initial decrease of the foam volume is due to the drainage of liquid out of the foam, Stage I in the figure; Stage II corresponds to slow narrowing of the Plateau borders at constant foam volume; further decrease of the foam volume, due to destruction of foam cells (Stage III), is observed if only a

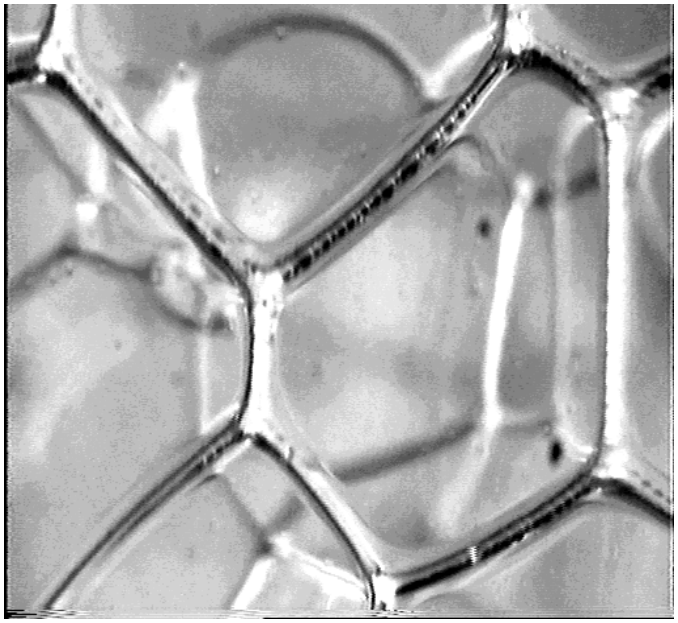

Fig. 14.7. Photograph of foam cells from Ref. [17]. Many oil drops entrapped in the Plateau borders can be seen. The experimental system is the same as in Fig. 14.6.

sufficient amount of silicone-oil emulsion is present in the solution; finally, the antifoaming action of the oil drops is completed and the foam volume levels off at a certain non-zero value, Stage IV in Fig. 14.6. A microscope view of the same foam at Stage II shows the presence of silicone oil drops entrapped in the Plateau borders, see Fig. 14.7, where a train of many captured oil drops is seen. Observation with a higher magnification reveals that the drops are certainly strongly compressed, since the walls of the Plateau border have acquired a wavy shape [17].

A different consequence of events is observed in systems with *fast* antifoaming action (from seconds to minutes). For example, Denkov et al. [18] formed foam from solution of the surfactant sodium dioctyl-sulfosuccinate (AOT) in the presence of antifoaming oil emulsion: poly-dimethyl-siloxane (PDMS) containing 4.2 wt% hydrophobized silica particles. A quick destruction of the foam is observed with this system. The investigation of separate films formed in the Scheludko cell show that before the expulsion of the oil drops out of the thinning film, some of them can "bridge" the two film surfaces, which appears as a typical interference pattern, called by the authors the "fish eye", see Fig. 14.8. Soon after the appearance of such "fish eyes" the foam film ruptures. With the help of a high-speed video-camera it was

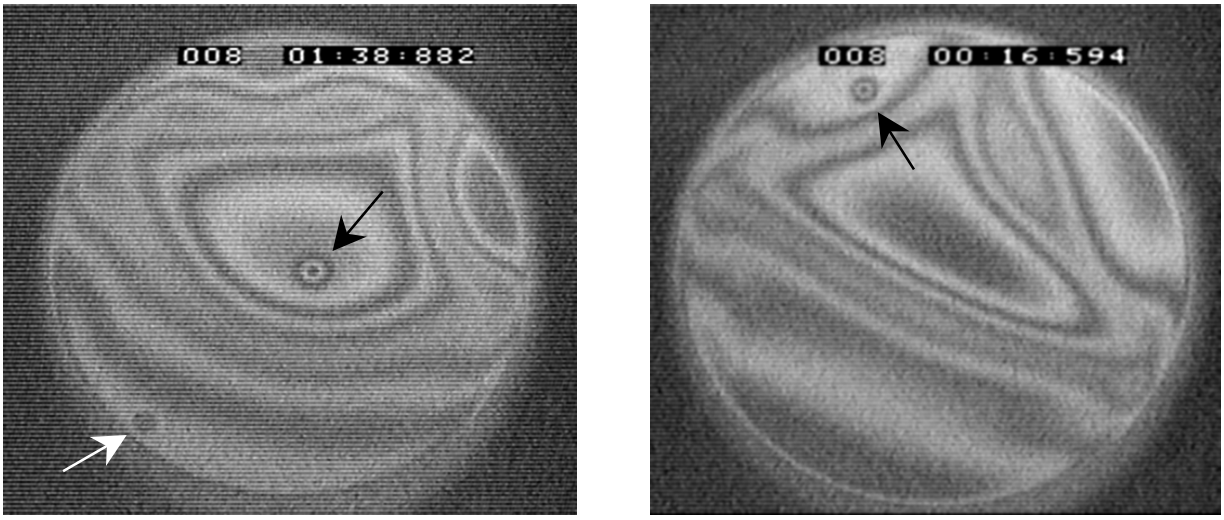

Fig. 14.8. Two video-frames taken by Denkov et al. [18] from a foam film formed in a Scheludko cell and observed in reflected light; interference fringes corresponding to zones of equal film thickness are seen. The foam films contain oil capillary bridges (shown by arrows), which look like "fish eyes" since they produce local concavities on the film surfaces. The films are made from AOT solution with 0.01 wt% added PDMS-emulsion; the latter contains 4.2 wt% hydrophobized silica particles

established that the “fish eye” indicates the formation of an oil capillary bridge with “neck” (see Chapter 11). Under certain conditions such a bridge becomes unstable: it spontaneously stretches and ruptures [18, 35]; for more details – see below.

In summary, the experiments show that the foam-breaking action of small oil drops can be located either in the foam films (Fig. 14.8) or in the Plateau borders (Figs. 14.6 and 14.7), depending on the specific system. It seems that the former situation is typical for systems with *fast* foam decay (less than a minute), whereas the latter situation is characteristic for *slowly* decaying foams (with lifetime from minutes to hours).

14.1.3. HYDRODYNAMICS OF DRAINAGE OF FOAM FILMS

A comprehensive review on hydrodynamics of drainage of liquid films can be found in Ref. [34]. At higher surfactant concentrations the liquid surface is occupied by a dense surfactant adsorption monolayer and it can be treated as *tangentially immobile*. At lower surfactant concentrations the hydrodynamic drag, due to the outflow of water, may create gradients of surfactant adsorption and surface tension, i.e. the *effect of Marangoni* takes place. In any case the fluid interfaces are deformable and their shape can change during the process of

thinning. The quantitative theoretical description requires a rather complicated mathematical treatment to be used [34,36], which is out of the scope of the present chapter.

It is instructive to consider a simpler case, which allows analytical solution. Imagine two plane-parallel and tangentially immobile film surfaces, which approach each other with a given velocity u. Let us assume that the two film surfaces are circular disks (of radius R) as it can be with the liquid films formed in the Scheludko cell, Fig. 14.2. The drainage of the liquid out of the gap (of width h) between such two disks is a classical problem solved by Reynolds [37,38]. If the film is thin ($h/R << 1$) and the velocity of drainage is small (small Reynolds number), the Navier-Stokes equation, connecting the pressure P inside the film and the velocity $\mathbf{v}$ of the draining water, acquires the following simpler form, known as the *lubrication approximation* [37,38]:

$$\frac{\partial^2 \mathrm{v}_r}{\partial z^2} = \frac{1}{\eta}\frac{\partial P}{\partial r}, \qquad \frac{\partial P}{\partial z} = 0 \qquad (h/R << 1) \tag{14.1}$$

Here η is the dynamic viscosity of the aqueous phase; the flow is assumed to have axial symmetry; r and z are the common cylindrical coordinates (along the radial and axial directions). Integrating Eq. (14.1), along with the boundary conditions at the film surfaces,

$$\mathrm{v}_r|_{z=0} = 0, \qquad \mathrm{v}_r|_{z=h} = 0 \qquad \text{(tangential immobility)}, \tag{14.2}$$

one obtains the distribution of the radial velocity across the film [37,38]:

$$\mathrm{v}_r = \frac{1}{2\eta}\frac{\partial P}{\partial r}\,(z^2 - hz) \tag{14.3}$$

which is related to the radial distribution of the pressure inside the draining film, $P(r)$. Further, we use the continuity equation for an incompressible fluid [38]:

$$\frac{\partial \mathrm{v}_z}{\partial z} = -\frac{1}{r}\frac{\partial (r\mathrm{v}_r)}{\partial r} \tag{14.4}$$

For v_z one can impose the following boundary conditions:

$$\mathrm{v}_z|_{z=0} = 0, \qquad \mathrm{v}_z|_{z=h} = -u \tag{14.5}$$

i.e. the lower surface is immobile, whereas the fluid at the upper film surface moves downwards with a given velocity u. Next we substitute Eq. (14.3) into Eq. (14.4) and integrate between $z = 0$ and $z = h$ using Eq. (14.5); the result reads [38]:

$$\frac{\partial}{\partial r}\left(r\frac{\partial P}{\partial r}\right) = -12\eta u\frac{r}{h^3} \tag{14.6}$$

Finally, we integrate Eq. (14.6), along with the boundary conditions

$$P(r{=}0) < \infty, \qquad P(r{=}R) = P_{\mathrm{PB}}\,, \tag{14.7}$$

to get the radial distribution of the pressure inside the film [37,38]:

$$P(r) = P_{\mathrm{PB}} + \frac{3\eta u}{h^3}(R^2 - r^2) \tag{14.8}$$

Here R is the radius of the foam film and P_{PB} is the pressure in the neighboring Plateau border. Equation (14.8) shows that the hydrodynamic pressure $P(r)$ in the center of the film ($r = 0$) is the highest. Similar is the situation when the deformability of the film surfaces is taken into account [34]. The highest pressure in the central part of a draining film is the reason for the appearance of a "dimple", see Fig. 14.4b. The above equations will be used in Section 14.3.3 to discuss the effect of evaporation on the breakage of foam films.

14.2. MECHANISMS OF FOAM-BREAKING ACTION OF OIL DROPS AND PARTICLES

14.2.1. SCHEME OF THE CONSECUTIVE STAGES

As mentioned earlier, knowing the mechanism of antifoaming action of colloid particles one can control the stability of foams, which could be regulated in the two opposite directions: stabilization or destabilization. Many combinations of foam-stabilizing surfactants and foam-breaking particles have been investigated. Different authors have proposed different mechanisms of antifoaming [4, 6, 18, 39-47]. Although there is no single universal mechanism, the accumulated experimental evidence implies the existence of several possible scenarios, which are summarized in Fig. 14.9.

The transition from state A to state B (Fig. 14.9) corresponds to drop (particle) *entry* at the surface of the liquid film. In the case of oil drop it is possible a molecularly thin film of oil to

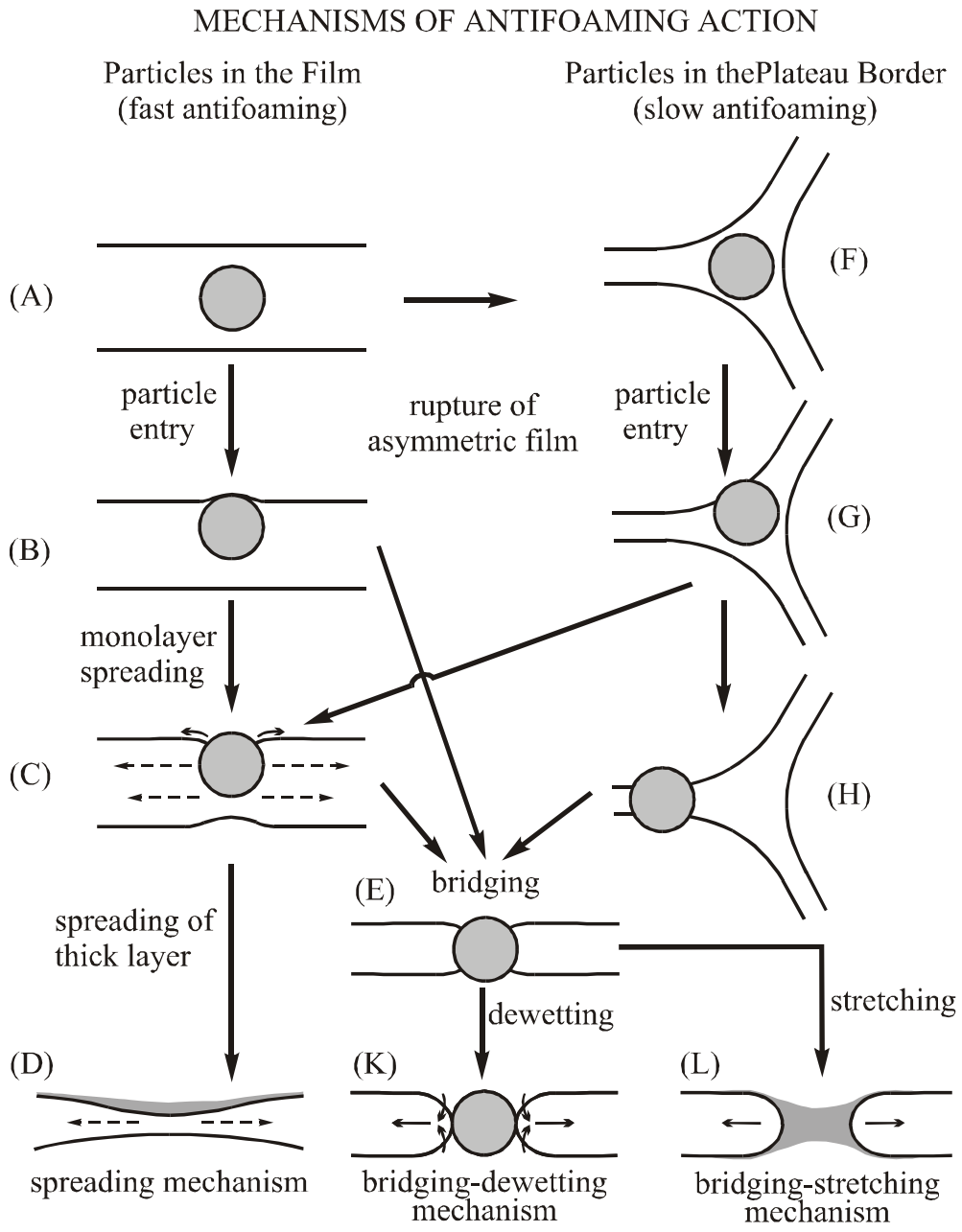

Fig. 14.9. Stages and transitions involved in the mechanisms of antifoaming action. The antifoam particle is schematically depicted as a sphere, but it can acquire a lens-shape if it is an oil drop. *Stage A*: particle in a foam film. *Stage B*: entry of a particle at the film surface. *Stage C*: spreading of a molecularly-thin oil film from an oil droplet. *Stage D*: spreading of a thick oil film (for positive spreading coefficient, $S > 0$), which leads to destabilization and rupture of the foam film. *Stage E*: bridging of the two film surfaces by an antifoam particle. *Stage F*: antifoam particle located in a Plateau border. *Stage G*: particle entry at one of the surfaces of the Plateau border. *Stage H*: particle entry at a second surface of the Plateau border. *Stage K*: dewetting of the formed "bridge" and rupture of the foam film. *Stage L*: Stretching of an oil bridge, which ruptures at its thinnest part and breaks the whole foam film.

spread over (or among) the hydrocarbon tails of the adsorbed surfactant molecules: this is the transition B→C in Fig. 14.9. The presence of molecular spreading can be established by measuring whether or not the surface tension exhibits a decrease after a small amount of oil is dropped on the surface of the surfactant solution. The propagation of the surface tension gradient, which accompanies the molecular spreading of oil, drives a water flow, which can locally accelerate the thinning of the foam film and can cause its destabilization and rupture. The molecular spreading (B→C) could be followed by a spreading of a thicker oil layer over the surface of the foam film (C→D). The latter leads to strong instabilities, manifested as irregular changes in the film thickness, which finally lead to rupturing of the film. The stages C and D (Fig. 14.9), followed by film rupture, represent the *spreading* mechanism of antifoaming action, proposed by Ross and McBain [39]; this mechanism has been observed and/or discussed by many authors [5,6,40-43]; for more details see Section 14.2.3 below.

The drop, lens or particle entry at one of the film surfaces could be followed by a second entry at the other film surface due to the thinning of the foam film, i.e. *bridging* could happen. This is the transition B→E in Fig. 14.9. The bridging could be accelerated by the spreading of oil monolayer, C→E. In the case of hydrophobic particle the bridging can be followed by dewetting, step E→K in Fig. 14.9, which eventually leads to breakage of the foam film. The sequence of stages E and K represents the *bridging-dewetting* mechanism, proposed by Garrett [44] and examined in many succeeding studies [4,15,23,45-47], see Section 14.2.4.

In the case of bridging by oil drops another scenario is also possible and experimentally observed [18,35]. An oil drop, bridging the surfaces of a foam film, is not spherical; it acquires the shape of a capillary bridge (see Chapter 11). A capillary bridge with “neck”, formed in a foam film, is usually unstable: the oil bridge begins to expand in lateral direction and to thin in its central part (stage L in Fig. 14.9), which soon leads to perforation of the bridge and rupture of the foam film. The sequence of stages E and L represents the *bridging-stretching* mechanism [18,35]. Note that oil capillary bridges with “haunch” (see Fig. 2.6) appear to be stable and do not break the foam film (unless oil spreading is also present). A criterion for determining whether or not the formation of an oil capillary bridge will cause rupturing of a foam film has been formulated by Garrett [45, 4] in terms of the so called *bridging coefficient*, see Eq. (14.11)

below. In Refs. [18,35] it has been established that the action of the investigated strong silicone antifoam follows the route A→B→E→L; see Section 14.2.5.

As pointed out in Section 14.1.2, in many cases the antifoaming particles (solid particulates or oil drops) can "peacefully" leave the foam film with the draining water, without producing any destabilizing effect (A→F in Fig. 14.9). Thus the particles are accumulated in the Plateau borders of the foam (stage F); see also Fig. 14.7. These particles could even have a transient foam-stabilizing action insofar as they hinder the water from leaving the foam through the Plateau borders [6]. In this way the drainage of water can be decelerated, but it cannot be prevented. As a result, the cross section of the Plateau borders progressively decreases, which brings about immobilization and pressing of the particles against the walls of the channel. This eventually leads to entry of some particle at one of the surfaces: see the transition F→G in Fig. 14.9; the latter takes much longer time compared to the transition A→B. As mentioned earlier, the transition A→B (entry in foam films) is pertinent to *fast* antifoaming, whereas the transition F→G (entry in Plateau borders) is typical for *slow* antifoaming. If the particle is a drop of oil, which can spread over the surface of the Plateau border and the neighboring films (transition G→C in Fig. 14.9), then the film rupturing can occur following the spreading mechanism (C→D). In fact, A→F→G→C→D is found [17] to be the route for destruction of shampoo-type foams by silicone oil droplets, which are added as a hair-conditioning agent, see Section 14.2.3 for details.

An alternative scenario is the transition G→H to occur (Fig. 14.9), i.e. the particle confined in the Plateau border to enter two of its three surfaces, see Ref. [6]. In this way the particle actually enters the periphery of the foam film, to whom the two surfaces belong. The latter is equivalent to an act of bridging, which may lead to rupture of the foam film by means of the bridging-dewetting or bridging-stretching mechanisms (E→K or E→L in Fig. 14.9).

If the particle is an oil droplet, after the first entry (stage G in Fig. 14.9) it acquires the shape of a lens. Then the bridging (G→H) can be realized as a coalescence of two oil lenses located at two different surfaces of the Plateau border. Such a mechanism of bridging has been observed by Wang et al. [48]. A necessary condition for this coalescence to happen is the oil-water-oil film, formed between two lenses upon contact, to be unstable. This can be achieved by the

addition of small silica crystallites, which spontaneously occupy the oil-water interface of the lenses and promote the breakage of the oil-water-oil film [48]. After the lens coalescence, the formed oil bridge leads to rupturing of the foam cell; the exact route has not been detected; it could be the bridging-stretching mechanism (E→L).

Knowing the diversity of combinations between foam-stabilizing surfactants and foam-destabilizing particles, one could not rule out the possibility for the existence of stages, transitions or mechanisms different from those mentioned above and illustrated in Fig. 14.9.

14.2.2. ENTERING, SPREADING AND BRIDGING COEFFICIENTS

Having in mind the variety of scenarios for the occurrence of the antifoaming action, it would be helpful if some criteria can allow one to foresee which is the most probable mechanism for a given system. All mechanisms presented in Fig. 14.9 involve the particle entry at the air-water interface as a necessary stage. Robinson and Woods [49] proposed a criterion for drop *entry* in terms of the surface tensions of the air-water, oil-water and oil-air interfaces, σ_{AW}, σ_{OW} and σ_{OA}, respectively:

$$E > 0, \qquad E \equiv \sigma_{AW} + \sigma_{OW} - \sigma_{OA} \qquad (E \text{ - entering coefficient}) \qquad (14.9)$$

A sufficient condition for spontaneous *spreading* of oil over the air-water interface was formulated by Harkins [50]:

$$S > 0, \qquad S \equiv \sigma_{AW} - \sigma_{OW} - \sigma_{OA} \qquad (S \text{ - spreading coefficient}) \qquad (14.10)$$

A criterion for instability of an oil *bridge* was formulated by Garrett [45]:

$$B > 0, \qquad B \equiv \sigma_{AW}^2 + \sigma_{OW}^2 - \sigma_{OA}^2 \qquad (B \text{ - bridging coefficient}) \qquad (14.11)$$

see Figs. 14.10 – 14.12. Below we discuss the physical meaning of the coefficients E, S and B, as well as their relation to the foam-breaking action of oil droplets.

As illustrated in Fig. 14.10, the particle entry is related to the disappearance of two interfaces of surface tensions σ_{AW} and σ_{OW}, and by the appearance of a new interface of tension σ_{OA}; this is reflected in the form of the definition of the entering coefficient E, Eq. (14.9). If $E > 0$, then the

$$E \equiv \sigma_{AW} + \sigma_{OW} - \sigma_{OA}$$

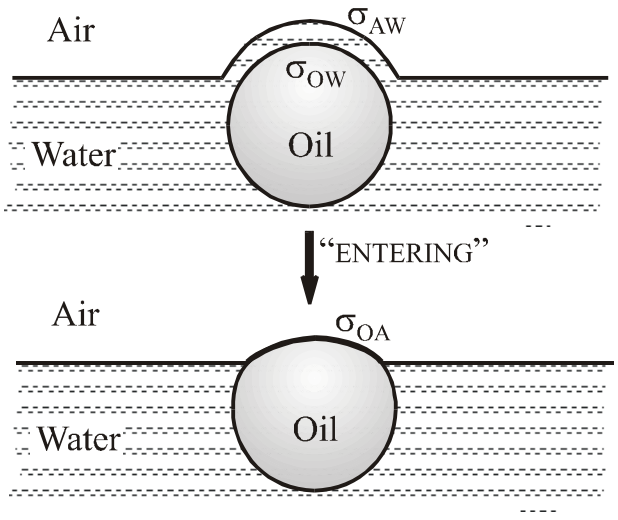

Fig. 14.10. The entering of an oil drop at the air-water interface leads to the disappearance of two interfaces of surface tensions σ_{AW} and σ_{OW}, and to the appearance of a new interface of tension σ_{OA}; this is reflected in the definition of the entering coefficient E. For $E > 0$ the entering could happen spontaneously if there is no high disjoining-pressure barrier to drop entry.

$$S \equiv \sigma_{AW} - \sigma_{OW} - \sigma_{OA}$$

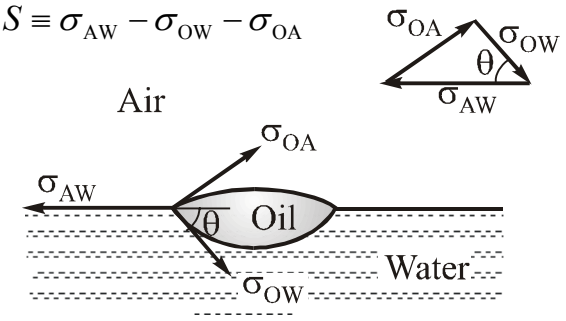

Fig. 14.11. A lens can rest in equilibrium on the air-water interface if only the Neumann triangle, formed by the vectors of the three interfacial tensions, σ_{AW}, σ_{OW} and σ_{OA}, exists. For $S > 0$ such a triangle does not exist; then one observes a spontaneous spreading of oil over the air-water interface, instead of lens formation.

$$B \equiv \sigma_{AW}^2 + \sigma_{OW}^2 - \sigma_{OA}^2$$

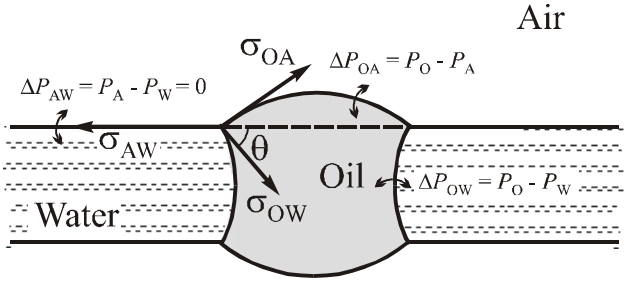

$$\theta < \pi/2 \Longrightarrow B > 0$$

Fig. 14.12. Sketch of an oil bridge formed inside a plane-parallel foam film. The bridge can rest in equilibrium if $\Delta P_{OW} = \Delta P_{OA}$. The latter requirement cannot be satisfied if $\theta < \pi/2$ as depicted in the figure; this corresponds to positive bridging coefficient, $B > 0$, see Eq. (14.12); in such a case the bridge has a non-equilibrium configuration and causes film rupture.

entry of the particle is energetically favorable. However, $E > 0$ does not guarantee drop entry. Indeed, a necessary condition for effectuation of drop entry is rupturing of the asymmetric oil-water-air film, separating the drop from the air-water interface. This asymmetric film could be stabilized by the action of electrostatic (double layer), steric or oscillatory structural forces [6], see Section 14.3.1 below. They create a barrier to drop entry, which can be manifested as existence of a maximum (or multiple maxima) in the disjoining pressure isotherm, see Chapter 5 for details. If this barrier is high enough, drop entry will not happen, despite the fact that it is energetically favorable ($E > 0$). This situation is analogous to an exothermic chemical reaction, which does not eventuate because of the existence of a high activation-energy barrier.

As an illustration, values of the entering coefficient E for a shampoo-type system are shown in Table 14.1; E has a minimum for a given surfactant composition (at Betaine molar fraction about 0.6), which is due to a synergistic effect for the used couple of surfactants [17]. For all compositions of this surfactant blend the entering coefficient E is positive (Table 14.1), which means that the oil-drop entry is energetically favorable; moreover, the other two coefficients are also positive: $S > 0$ and $B > 0$. However, in this system the oil drops exhibit only a weak and slow antifoaming action [17], which indicates the existence of a barrier to drop entry, as discussed above.

An oil drop located at the air-water interface acquires a lens-shape, Fig. 14.11. Such a lens can rest in equilibrium if only the Neumann triangle, formed by the three interfacial tensions, σ_{AW}, σ_{OW} and σ_{OA}, does exist (see Chapter 2 for details). As known, such a triangle cannot exist if one of its sides is longer than the sum of the other two sides, say $\sigma_{AW} > \sigma_{OW} + \sigma_{OA}$, that is $S > 0$, see Eq. (14.10). If the spreading coefficient is positive ($S > 0$), one observes a spontaneous spreading of the oil over the air-water interface; in contrast, negative spreading coefficient ($S < 0$) corresponds to the formation of equilibrium oil lenses [51].

Often the sign of S depends on whether the interface is preequilibrated with the oil phase (see e.g. Table 14.1): S could be positive for a non-preequilibrated interface, whereas S could become negative after the equilibration. This is due to the decrease of σ_{AW} caused by the molecular spreading of oil. The values of σ_{AW} "without oil" and "equilibrated with oil" in

Table 14.1. Measured interfacial tensions and calculated entering, spreading and bridging coefficients, E, S and B; S_{eq} is the spreading coefficient after the equilibration with oil. The data are obtained in Ref. [17] for mixed surfactant solutions of Betaine (dodecyl-amide-propyl betaine) and SDP3S (sodium dodecyl-trioxyetylene-sulfate) at total concentration 0.1 M; the hydrophobic phase is silicon oil.

Molar part of Betaine	σ_{OA} mN/m	σ_{OW} mN/m	σ_{AW} mN/m (no oil)	σ_{AW} mN/m (equilibrated with oil)	E mN/m	S mN/m	B $(mN/m)^2$	S_{eq} mN/m
0.0	19.8	8.45	32.7	25.5	21.4	4.45	749	–2.75
0.2	19.8	7.10	30.4	23.9	17.7	3.50	582	–3.00
0.4	19.8	6.40	29.0	23.0	15.6	2.80	490	–3.20
0.5	19.8	5.70	28.9	23.1	14.8	3.40	476	–2.40
0.6	19.8	5.50	28.8	23.1	14.5	3.50	468	–2.20
0.8	19.8	5.70	29.0	23.5	14.9	3.50	482	–2.00
1.0	19.8	6.65	31.6	26.3	18.5	5.15	651	–0.15

Table 14.1 are measured, respectively, before and after dropping locally a small amount of oil on the surface of the investigated surfactant solution. Note that $S > 0$ automatically implies $E > 0$, cf. Eqs. (14.9) and (14.10). On the other hand, a high barrier to drop entry can prevent both the drop entering and the subsequent spontaneous spreading of oil.

To introduce the bridging coefficient B, Garrett [45] considered the balance of the pressures in the case of an oil capillary bridge formed in a foam film, Fig. 14.12. For the sake of simplicity it was assumed, that the film (air-water) surfaces are plane-parallel. Then the pressure change across the air-water interface is (approximately) equal to zero, that is $\Delta P_{AW} \equiv P_A - P_W = 0$. The latter fact implies, that the pressure differences across the oil-water ($\Delta P_{OW} \equiv P_O - P_W$) and oil-air ($\Delta P_{OA} \equiv P_O - P_A$) interfaces must be approximately equal, i.e. $\Delta P_{OW} \approx \Delta P_{OA}$, for an equilibrium bridge.

The latter requirement certainly cannot be satisfied if the oil-air interface is *convex* ($\Delta P_{OA} > 0$), whereas the oil-water interface is concave ($\Delta P_{OW} < 0$), see Fig. 14.12. Hence, such a bridge cannot be in mechanical equilibrium, and its destruction will cause rupturing of the foam film. As seen in Fig. 14.12 this non-equilibrium configuration corresponds to $\theta < \pi/2$, that is to $\cos\theta > 0$. This is the same angle θ, which appears in the Neumann triangle in Fig. 14.11. Using the cosine theorem for this triangle one obtains [45]:

$$B \equiv \sigma_{AW}^2 + \sigma_{OW}^2 - \sigma_{OA}^2 = 2\sigma_{AW}\,\sigma_{OW}\cos\theta \tag{14.12}$$

Then it is obvious that the condition for non-equilibrium configuration, $\cos\theta > 0$, is equivalent to $B > 0$, cf. Eq. (14.11). On the other hand, an equilibrium configuration is possible when both the oil-air and oil-water interfaces are convex, and consequently $\Delta P_{OW} = \Delta P_{OA} > 0$. One may check that this configuration corresponds to $\cos\theta < 0$ and $B < 0$.

For the sake of simplicity let us denote $x \equiv \sigma_{AW}$, $y \equiv \sigma_{OW}$ and $z \equiv \sigma_{OA}$. Then, in view of Eq. (14.12) the relationship $B > 0$ can be presented in the following equivalent forms:

$$B \equiv x^2 + y^2 - z^2 > 0 \quad \Leftrightarrow \quad (x+y)^2 - z^2 > 2xy \quad \Leftrightarrow \tag{14.13}$$

$$(x+y+z)(x+y-z) > 2xy \quad \Leftrightarrow \quad (x+y+z)E > 2xy \tag{14.14}$$

where at the last step we used the definition of the entering coefficient E, Eq. (14.9). Since x, y and z are positive, Eq. (14.14) implies that E must be also positive. In other words, from $B > 0$ it follows $E > 0$, [52]. On the other hand, from $E > 0$ it does not necessarily follow $B > 0$.

The experiment shows, that sometimes bridges with $B > 0$ can be (meta)stable (like the "fish eyes" in Fig. 14.8) in contrast with the prediction of the criterion Eq. (14.11). This can be due to the fact that in reality the foam film is not plane-parallel in a vicinity of the oil bridge [35], as it is assumed when deriving Eq. (14.11).

The data in Table 14.1 shows that for a shampoo-type system all three coefficients are positive ($E > 0$, $S > 0$ and $B > 0$), and one could expect that the drop entry and oil spreading occur spontaneously, and the formed oil bridges are unstable. In contrast, the experiment shows that the oil drops in this system exhibit a rather weak antifoaming action. As already discussed, this apparent discrepancy can be attributed to the existence of a high disjoining pressure barrier to

drop entry. Note that the drop (particle) entry is a necessary step in each of the antifoaming mechanisms shown in Fig 14.9. Hence, the information about E, S and B should be combined with data about the stability of the asymmetric oil-water-air films in order to predict the antifoaming activity for a given system [6, 17].

14.2.3. SPREADING MECHANISM

As mentioned earlier, after entering the air-water interface an oil drop forms a lens. At the same time, spreading of a molecularly thin oil film can happen. If the spreading coefficient is positive ($S > 0$), then spontaneous spreading of thick oil film could also happen, which would strongly destabilize the foam films.

The foam-destabilizing action of oil spreading was pointed out in the studies by Ross and McBain [39] and Ross [40], in which the spreading mechanism was formulated. It was noted there that the spreading may lead to bridging. As a possible scenario it has been suggested that the foam-destructive role of oil consists in spreading of an oil duplex film on both sides of the foam film, thereby driving out the aqueous phase and leaving an oil film, which is unstable and easily breaks [39]. The importance of oil spreading for the antifoaming action has been emphasized in subsequent works [41-43, 49, 53-59]. Kulkarni et al. [5] have noted, that the major advantage of the silicone antifoams over their organic counterparts arises by virtue of the low surface tension and spontaneous spreading of the silicone oil over most aqueous foaming systems. The organic oils, in general, cannot spread effectively on aqueous surfactant solutions, on which, on the other hand, the silicone oils have positive spreading coefficient ($S > 0$) [5].

The mechanism of foam destruction by silicone-oil droplets in a shampoo-type system has been directly observed by Basheva et al. [17] in experiments with vertical films formed in the three-leg frame, see Fig. 14.3. Silicone-oil droplets of average size 11 μm (volume fraction 0.001 in the emulsion) have been dispersed in 0.1 M solution of sodium dodecyl-trioxyethylene sulfate (SDP3S). After the simultaneous creation of three vertical films in the frame, one first observes their regular thinning (Fig. 14.13a). The oil droplets are expelled from the foam films and accumulated in the Plateau border (Fig. 14.13b). The Plateau border also thins due to the drainage of water. At a certain moment one observes entry of an oil drop at the surface of the

Plateau border, which is accompanied by a fast oil spreading over the neighboring foam films (Fig. 14.13c). The spreading of oil causes hydrodynamic instabilities, which quickly propagate over the whole film area (Fig. 14.13d). The film ruptures several seconds after the drop entry.

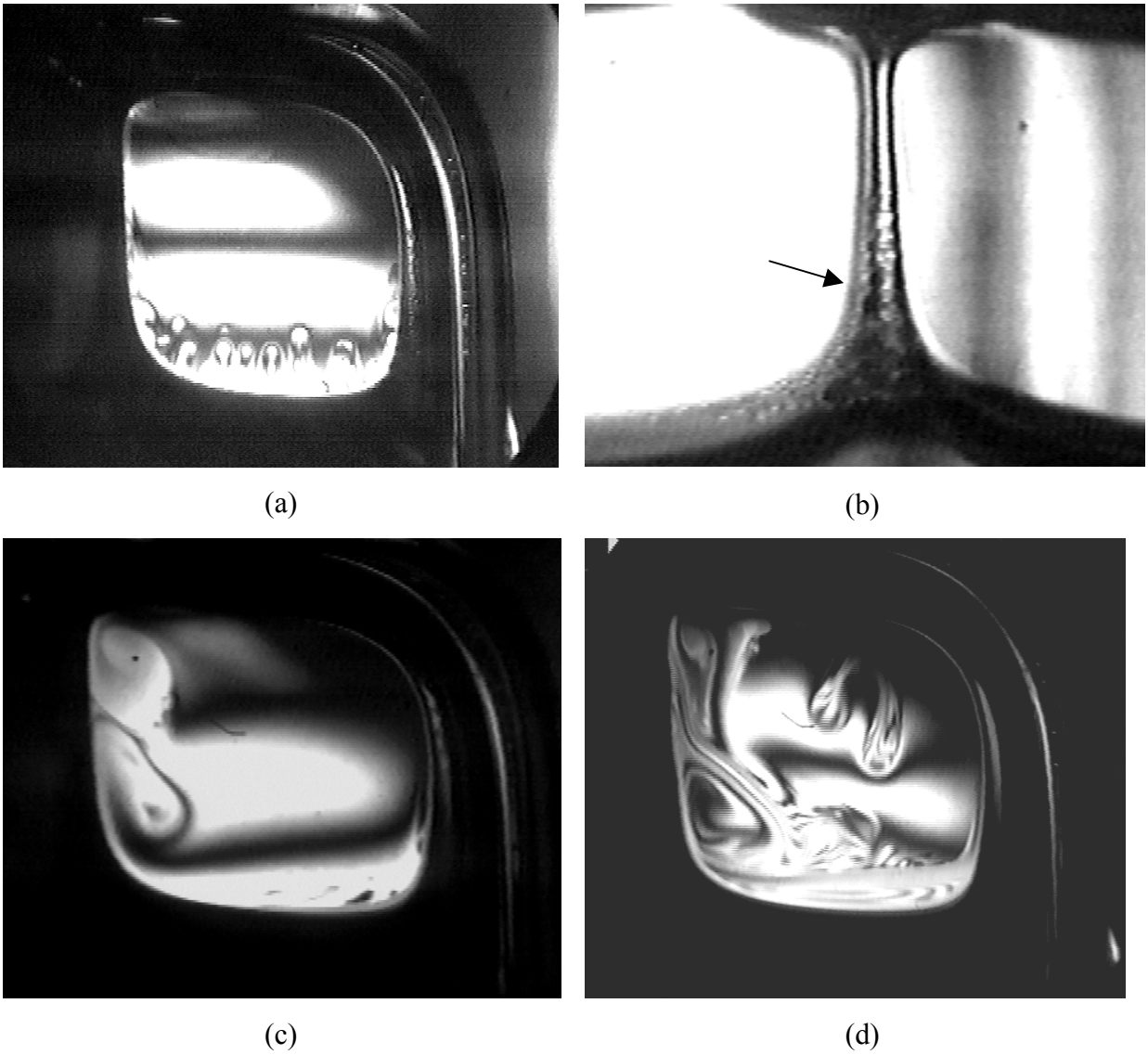

Fig. 14.13. Vertical films formed in a three-leg frame (see Fig. 14.3): consecutive video-frames taken by Basheva et al. [17]. The films are produced from 0.1 M solution of SDP3S containing silicone-oil droplets of average size 11 μm. (a) Initially, the foam films are regularly thinning. (b) The oil droplets are expelled from the films and accumulated in the Plateau border, which also thins due to the outflow of water. (c) At a certain moment, an oil drop is observed to enter the surface of the Plateau border and spreading of oil over the neighboring foam films takes place. (d) This causes hydrodynamic instabilities followed by film rupture.

Consequently, in this system the antifoaming mechanism follows the route A→F→G→C→D in Fig. 14.9.

Although the importance of oil spreading has been widely recognized, many authors notice that there is no simple correlation between spreading and antifoaming action [4-6]. Many materials spread without showing antifoaming action, whereas others do not spread but nevertheless exhibit a foam-destructive effect. This situation is understandable having in mind the sequence of stages in the antifoaming mechanisms (Fig. 14.9). Indeed, since entering is a prerequisite for spreading, an oily material with high positive spreading coefficient cannot exhibit its antifoaming activity if there is a high barrier to oil-drop entry. On the other hand, non-spreading materials can have foam-breaking performance, insofar as there are other antifoaming mechanisms, alternative to spreading, like the bridging-dewetting and bridging-stretching mechanisms.

14.2.4. BRIDGING-DEWETTING MECHANISM

As already mentioned, the possibility for bridging of foam films by antifoam particles has been discussed long ago by Ross and McBain [39]. As a separate mechanism, especially for hydrophobic solid particles alone, the bridging-dewetting mechanism (the transition E→K in Fig. 14.9) was formulated by Garrett [44, 45], and was accepted in many subsequent studies for the cases of solid and liquid particles [4, 6, 15, 23, 46, 47].

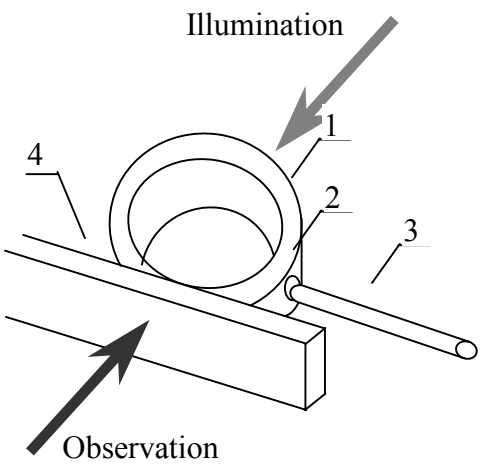

Fig. 14.14. Experimental cell used by Dippenaar [46] to study the rupture of liquid films by solid particles. A liquid film is formed in the interior of a short glass capillary (1) initially filled with aqueous solution. The thickness of the formed film is controlled by sucking or injection of liquid through the side orifice (2) and syringe-needle (3). The formed film is observed in transmitted light through the optical glass plate (4) to avoid the aberration due to the cylindrical wall. The cell is closed in container (not shown) to prevent evaporation of water and convection of air.

Dippenaar [46] directly recorded bridging-dewetting events with hydrophobic particles in water films (without surfactant) with the help of high-speed cinematography. In his experiments he used a version of the Scheludko cell, made of glass, whose cylindrical wall is optically connected to a vertical plane-parallel glass plate (Fig. 14.14). The observation of the foam films across the latter plate allows one to avoid optical distortions due to the cylindrical wall of the cell.

In the case of liquid antifoaming particles it was suggested [6, 15, 23, 33, 47, 60] that the lens, formed after the oil-drop entry at the air-water interface (in the film or Plateau border), enters also the opposite air-water surface, which leads to the formation of an oil bridge. Alternatively, such a bridge can be created by breaking of the oil-water-oil film formed between two lenses, attached to two air-water interfaces, as it is in the experiments of Wang et al. [48].

Fig. 14.15. An oil lens, initially attached to the upper film surface, enters the lower film surface. The Laplace pressure in the contact zone drives the liquid away from the lens thus dewetting its lower surface.

As a rule the foam systems contain surfactants, which adsorb at any hydrophobic surfaces rendering them hydrophilic. For that reason one can expect that the surface of any antifoam particle is hydrophilized by the surfactant. In other words, the surfactant promotes wetting (rather than dewetting) of antifoam-particles. In spite of that, the bridging by a hydrophilized oily drop can have a foam-destructive effect. The curvature of the film surfaces in the neighborhood of a bridging oil lens gives rise to a capillary pressure, which drives the water away from the lens (Fig. 14.15), until finally the two three-phase contact lines coincide. This is equivalent to dewetting of the oil lens, which is immediately followed by hole formation and film rupture [4, 17, 47]. Alternatively, the oil bridge *itself* can be mechanically unstable and can break in its central part after stretching (without dewetting), see Section 14.2.5.

14.2.5. BRIDGING-STRETCHING MECHANISM

Ross [40] mentioned the bridging-stretching mechanism (the transition E→L in Fig. 14.9) as one of the possible scenarios of foam destruction by oily drops. The existence of this mechanism was directly proven and experimentally investigated by Denkov et al. [18, 35] with the help of a high-speed video camera (1000 frames per second). Foam films with oily bridges were formed in the experimental cell of Dippenaar (Fig. 14.14) in the following way [18, 35]:

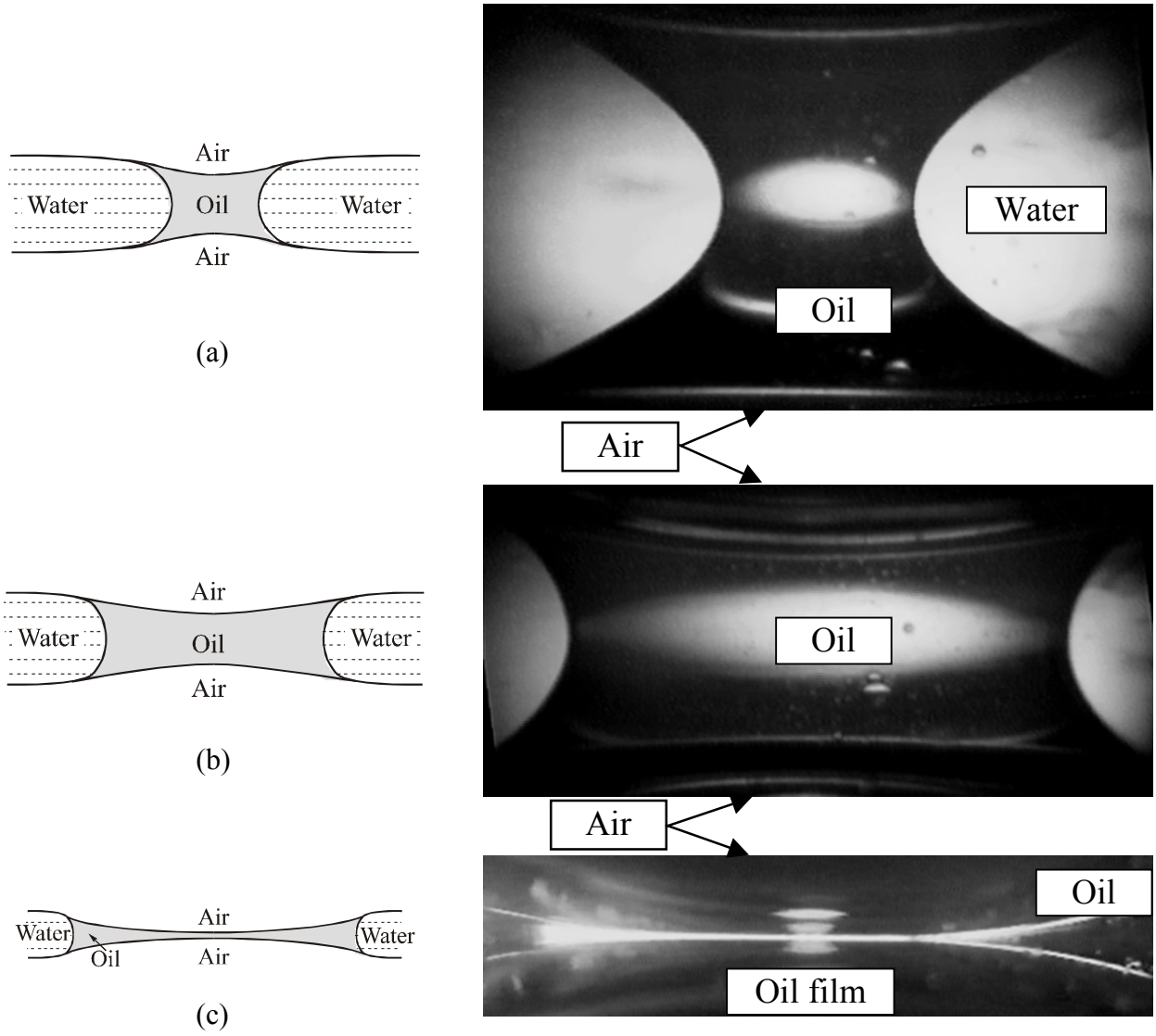

Fig. 14.16. Sketch of the system configuration (on the left) and consecutive video-frames (on the right) of an oil capillary bridge formed in a foam film; experimental results of Denkov et al. [18]. (a) A capillary bridge with "neck" is formed after an oil lens, situated at the upper surface of the aqueous layer, touches its lower surface. (b) The capillary bridge stretches with time. (c) Unstable oil film appears in its central zone, which ruptures breaking the whole foam film.

First the cylindrical experimental cell has been loaded with the investigated aqueous surfactant solution, which acquires the shape of a biconcave liquid layer. Then an oil drop (of diameter about 100 μm) is placed on the upper concave meniscus; the oil forms a floating lens situated in the central zone of the meniscus. Next, some amount of the aqueous solution is gradually sucked out from the biconcave liquid layer, which leads to a decrease of its thickness. An oil capillary bridge forms when the oil lens situated at the upper surface of the aqueous layer touches its lower surface (Fig. 14.16a). The observations show that this capillary bridge stretches with time (Fig. 14.16b) and an oily film appears in its central zone (Fig. 14.16c). The oily film is unstable: it ruptures and breaks the whole foam film. The total period of existence of these unstable oil bridges in foam films is only several milliseconds [18, 35].

It is worthwhile noting that the oil capillary bridges of relatively small size turn out to be mechanically stable. On the other hand, the larger bridges are unstable. This behavior is consonant with the theoretical predictions [35]. Initially small stable bridges could be latter transformed into unstable ones due to the action of the following two factors.

(i) The characteristic length, determining whether a capillary bridge is small or large, is scaled by the thickness of the foam film; when the thickness (the length scale) decreases due to the drainage of water an oily bridge of fixed volume may undergo a transition from small stable into large unstable.

(ii) It has been established [35] that oil can be transferred from a pre-spread oil layer (over the air-water interface) toward the oil bridge; thus the size of the bridge actually increases and it can undergo a transition from stable state to unstable state.

In the experiments by Denkov et al. [18, 35] the lifetime of the small *stable* bridges has been up to several seconds; this is the time elapsed between the moments of bridge formation and destabilization. As already mentioned, the lifetime of the larger *unstable* bridges is only few milliseconds and it can be recorded with the help of a high-speed video technique. The latter enables one to establish whether the oil bridge ruptures the film following the stretching or dewetting mechanisms.

14.3. STABILITY OF ASYMMETRIC FILMS: THE KEY FOR CONTROL OF FOAMINESS

14.3.1. THERMODYNAMIC AND KINETIC STABILIZING FACTORS

The formation of a stable or unstable foam depends on the stability of the separate *air-water-air* films. In addition, a colloidal particle (say, an oil droplet) can exhibit antifoaming action if only the asymmetric *particle-water-air* film is unstable. The rupture of the latter film is equivalent to particle entry, which is a necessary step of the spreading and bridging mechanisms (Fig. 14.9). Consequently, the stability of the respective liquid films has a primary importance for both foamability and antifoaming action. The factors, which govern the stability, are similar for symmetric and asymmetric liquid films; these factors, and the related mechanisms of film rupture, are considered below in this section.

The major *thermodynamic stabilizing factor* is the action of a repulsive disjoining pressure, Π, within the liquid film. A stable equilibrium state of a liquid film can exist if only the following two conditions are satisfied [61]:

$$\Pi = P_{\mathrm{A}} \qquad \text{and} \qquad \left(\frac{\partial \Pi}{\partial h}\right)_{\Pi = P_{\mathrm{A}}} < 0 \ . \tag{14.15}$$

As usual, h denotes the film thickness, and P_{A} is the pressure difference applied across the surface of the film. For example, if one of the film surfaces represents a liquid-gas interface one can write [62]

$$P_{\mathrm{A}} \approx P_g - P_l + 2\sigma_{lg}/R_f \tag{14.16}$$

where P_l and P_g is the pressure in the bulk liquid and gas phases, respectively; R_f is the radius of curvature of the film surface, and σ_{lg} is its surface tension (see Chapter 5). For a flat film ($R_f \to \infty$) one has simply $P_{\mathrm{A}} = P_g - P_l$. Note that for oil droplets captured in foams the asymmetric oil-water-air films are curved and the term $2\sigma_{lg}/R_f$ in Eq. (14.16) must be taken into account. The condition $\Pi = P_{\mathrm{A}}$ means that at equilibrium the disjoining pressure Π counterbalances the pressure difference P_{A} applied across the film surface. In addition, the condition $\partial\Pi/\partial h < 0$ guarantees that the equilibrium is stable (rather than unstable).

(a) Electrostatic DLVO Barrier (b) Multiple Barriers Due to Micelles

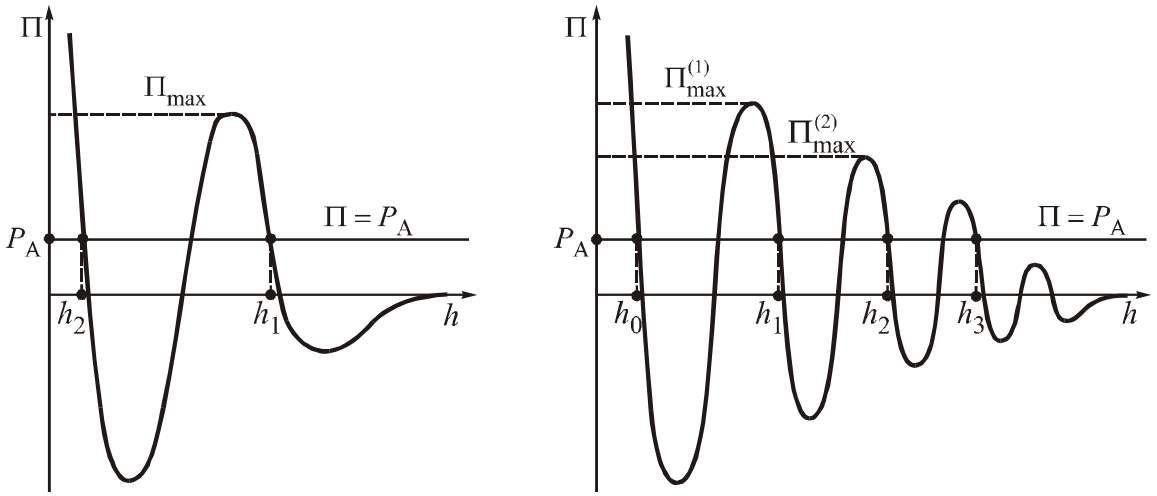

Fig. 14.17. Typical plots of disjoining pressure Π vs. film thickness h; P_A is the pressure difference applied across the film surface; the equilibrium states of the liquid film correspond to the points in which $\Pi = P_A$. (a) DLVO-type disjoining pressure isotherm $\Pi(h)$; the points at $h = h_1$ and h_2 correspond to primary and secondary films, respectively; Π_{max} is the height of a barrier due to the electrostatic repulsion between the film surfaces. (b) The presence of surfactant micelles (or other monodisperse colloidal particles) give rise to an oscillatory structural force between the two surfaces of a liquid film; the disjoining pressure isotherm $\Pi(h)$ exhibits multiple decaying oscillations; the stable equilibrium films with thickness h_0, h_1, h_2 and h_3 correspond to films containing 0, 1, 2 and 3 layers of micelles, respectively.

As an illustration, Fig. 14.17a shows a typical DLVO-type disjoining pressure isotherm $\Pi(h)$, see Chapter 5 for more details. There are two points, $h = h_1$ and $h = h_2$, at which the condition for stable equilibrium, Eq. (14.16), is satisfied. In particular, $h = h_1$ corresponds to the so called *primary film*, which is stabilized by the electrostatic (double layer) repulsion. The addition of electrolyte to the solution may lead to a decrease of the height of the electrostatic barrier, Π_{max} [61, 63]; at high electrolyte concentration it is possible to have $\Pi_{max} < P_A$; then primary film does not exist.

The equilibrium state at $h = h_2$ (Fig. 14.17a) corresponds to a very thin *secondary film*, which is stabilized by the short-range Born repulsion. The secondary film represents a bilayer of two adjacent surfactant monolayers; its thickness is usually about 5 nm (slightly greater than the doubled length of the surfactant molecule) [64]. Secondary films are observed in stable "dry foams" formed after the drainage of most of the water out of the foam.

The situation is more complicated when the aqueous solution contains surfactant micelles, which is a very common situation in practice. In such a case the disjoining pressure isotherm $\Pi(h)$ can exhibit multiple decaying oscillations, whose period is close to the diameter of the micelles (Fig. 14.17b); see Section 5.2.7 above. The condition for equilibrium liquid film, Eq. (14.15), can be satisfied in several points, denoted by h_0, h_1, h_2 and h_3 in Fig. 14.17b; the corresponding films contain 0, 1, 2 and 3 layers of micelles, respectively. The transitions between these multiple equilibrium states represent the phenomenon *stratification*, see Refs. [30, 65-76]. The presence of disjoining pressure barriers, which are due either to the electrostatic repulsion (Fig. 14.17a), or to the oscillatory structural forces (Fig. 14.17b), has a stabilizing effect on liquid films and foams.

The existence of a stable equilibrium state (cf. Fig. 14.17) does not guarantee that a draining liquid film can "safely" reach this state. Indeed, the hydrodynamic instabilities, accompanying the drainage of the water, could rupture the film before it has reached its thermodynamic equilibrium state [77]. There are several *kinetic stabilizing factors*, which suppress the hydrodynamic instabilities and decelerate the drainage of the film, thus increasing its life-time. Such a factor is the *Gibbs (surface) elasticity* of the surfactant adsorption monolayers; it tends to eliminate the gradients in adsorption and surface tension (the Marangoni effect) and damps the fluctuation capillary waves. At high surfactant concentrations the Gibbs elasticity is also high and it renders the interface tangentially immobile, see e.g. [78]. The *surface viscosity* also impedes the drainage of water out of the films because of the dissipation of a part of the kinetic energy of the flow within the surfactant adsorption monolayers. The *surfactant adsorption relaxation time* (see Chapter 1) is another important kinetic factor. In the process of foam formation a new water-air interface is created. If the adsorption relaxation time is small enough, a dense adsorption monolayer will cover the newly formed interface and will protect the gas bubbles against coalescence upon collision. In the opposite case (slow adsorption kinetics) the bubbles can merge upon collision and the volume of the created foam (if any) will be relatively small.

14.3.2. MECHANISMS OF FILM RUPTURE

The role of the foam stabilizing (or destabilizing) factors can be understood if the mechanism of film rupture is known. Several different mechanisms of rupture of liquid films have been proposed, which are briefly described below.

(a) Fluctuation Capillary Waves in relatively thick films; de Vries (1958)

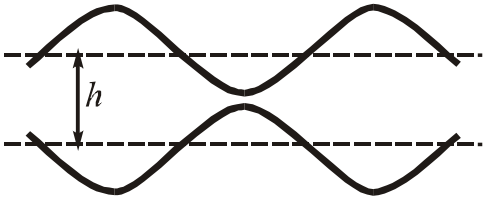

(b) Nucleation of Pores in thin bilayer films; Derjaguin & Gutop (1962)

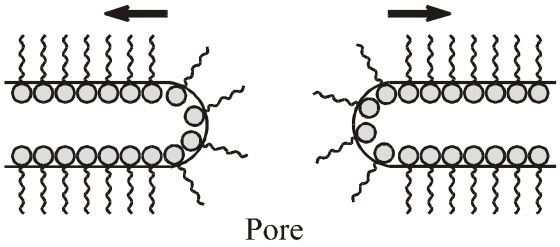

(c) Transport of Solute across the Film Marangoni instability; Ivanov et al. (1987)

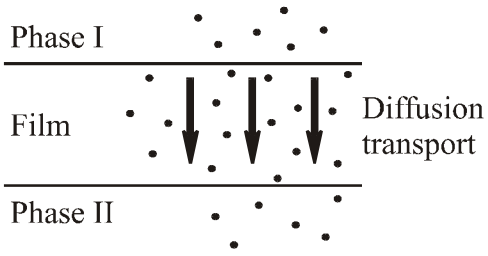

Fig. 14.18. Mechanisms of rupturing of liquid films. (a) Fluctuation-wave mechanism: the film rupture is a result of growth of capillary waves enhanced by attractive surface forces. (b) Pore-nucleation mechanism: it is expected to be operative in very thin films, representing two attached monolayers of amphiphilic molecules. (c) Solute-transport mechanism: if a solute is transferred across the two surfaces of the liquid film due to chemical-potential gradients, it may provoke Marangoni instability and film rupture.

The most popular is the *capillary-wave mechanism* proposed by de Vries [79] and developed in subsequent studies [80-85, 36, 78], see Fig. 14.18a. The conventional version of this mechanism is developed for the case of monotonic attraction between the two surfaces of the liquid film (say, van der Waals attraction). Thermally excited fluctuation capillary waves are always present at the film surfaces. With the decrease of the average film thickness, h, the attractive disjoining pressure enhances the amplitude of some modes of the fluctuation waves. At a given critical value of the film thickness, h_{cr} , corrugations on the two opposite film surfaces can touch each other and then the film will break [36]. The critical thickness of a film having area πR^2 can be estimated using the following relationship [81, 78]:

$$\frac{2R^2}{\sigma}\left(\frac{\partial \Pi}{\partial h}\right) \geq j_1^2 = 5.783... \tag{14.17}$$

where j_1 is the first zero of the Bessel function J_0; as usual, σ denotes surface tension. The relationship (14.17) can be satisfied only for positive $\partial\Pi/\partial h$. In the special case of van der Waals interaction one can substitute $\partial\Pi/\partial h = A_H/(2h^4)$, where A_H is the Hamaker constant; then Eq. (14.17) shows that the critical thickness increases with the increase of the film radius R, i.e. the films of larger area break easier (at a greater thickness) than the films of smaller area. An estimate for the critical thickness of the film *between two bubbles* of radius a is available [78]:

$$h_{cr} \approx \left(\frac{aR^2 A_H^2}{288\pi^2\sigma^2}\right)^{1/7} \tag{14.18}$$

Equation (14.18) is found to agree well with experimental data for h_{cr} vs. R. The effect of kinetic factors, such as the surface viscosity, elasticity and diffusivity are taken into account in Refs. [36, 78, 83-85].

The mechanism of *film rupture by nucleation of pores* has been proposed by Derjaguin and Gutop [86] to explain the braking of very thin films, built up from two attached monolayers of amphiphilic molecules. Such are the secondary foam films and the bilayer lipid membranes. This mechanism was further developed by Derjaguin and Prokhorov [61, 87, 88], Kashchiev and Exerowa [89-91], Chizmadzhev et al. [92-94], Kabalnov and Wennerström [95]. The formation of a nucleus of a pore (Fig. 14.18b) is favored by the decrease of the surface energy, but it is opposed by the edge energy of the pore periphery. The edge energy can be described (macroscopically) as a line tension [87-91], or (micromechanically) as an effect of the spontaneous curvature and bending elasticity of the amphiphilic monolayer [95]. For small nuclei the edge energy is predominant, whereas for larger nuclei the surface energy gets the upper hand. Consequently, the energy of pore nucleation exhibits a maximum at a given *critical* pore size; the larger pores spontaneously grow and break the film, while the smaller pores shrink and disappear.

A third mechanism of liquid-film rupture is observed when there is a *transport of solute across the film*, see Fig. 14.18c. This mechanism, investigated experimentally and theoretically by

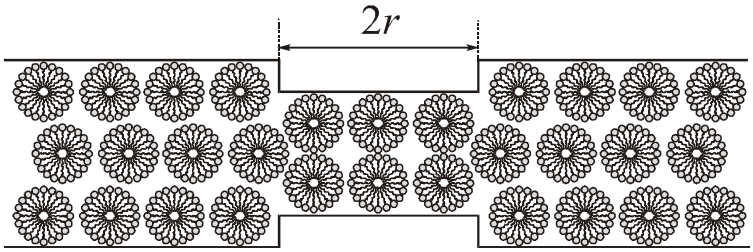

Fig. 14.19. The formation of spots of lower thickness in stratifying liquid films could be attributed to condensation of vacancies in the colloid-crystal-like structure of surfactant micelles formed inside the liquid film [68]; r denotes the spot radius.

Ivanov et al. [96-98], was observed with emulsion systems (transfer of alcohols, acetic acid and acetone across liquid films), but it could appear also in some asymmetric oil-water-air films. The diffusion transport of some solute across the film leads to the development of Marangoni instability, which manifests itself as a forced growth of capillary waves at the film surfaces and eventual film rupture. Note that Marangoni instability can be caused by both mass and heat transfer [98-101]. In the case of oils, which are soluble in water, the instability could be caused by surface tension gradients due to the diffusion transport of oil to the water-air interface [102].

A fourth mechanism of film rupture is the *barrier mechanism*. It is directly related to the physical interpretation of the equilibrium states in Fig. 14.17. For example, let us consider an electrostatically stabilized film of thickness h_1 (Fig. 14.17a). Some processes in the system may lead to the increase of the applied capillary pressure P_A. For example, if the height of a foam column increases from 1 cm to 10 cm, the hydrostatic effect increases the capillary pressure in the upper part of the foam column from 98 Pa up to 980 Pa. Thus P_A could become greater than the height of the barrier, Π_{max}, which would cause either film rupture, or transition to the stable state of secondary film at $h = h_2$ (Fig. 14.17a). The latter two possibilities could be realized with different probability, say 80 % of the films may rupture and 20 % of the films may safely reach the next equilibrium state of secondary film, see e.g. Ref. [103]. The increase of the adsorption density stabilizes the secondary films. In addition, the decrease of Π_{max} decreases the probability the film to rupture after the barrier is overcome. Indeed, the overcoming of the barrier is accompanied with a violent release of mechanical energy accumulated during the increase of P_A. If the barrier is high enough, the released energy could break the liquid film. On the other hand, if the barrier is not too high, the film could survive the transition.

14.3.3. OVERCOMING THE BARRIER TO DROP ENTRY

In reality, the overcoming of the barrier can be facilitated by various factors. Most frequently the transition happens trough the formation and expansion of spots of lower thickness within the film (Fig. 2.11b), rather than by a sudden decrease of the thickness of the whole film. Physically this is accomplished by a nucleation of spots of sub-μm size, which resembles a transition with a "tunnel effect", rather than a real overcoming of the barrier. A theoretical model of spot formation in stratifying films by condensation of vacancies in the structure of ordered micelles (see Figs. 14.17b and 14.19) has been developed in Ref. [68]. The nucleation of spots makes the transitions less violent and decreases the probability for film rupturing. The increase of the applied capillary pressure P_A facilitates the spot formation and the transition to state with lower film thickness; this has been established by Bergeron and Radke [71], who experimentally obtained portions of the stable branches of the oscillatory disjoining-pressure curve (Fig. 14.17b).

Other factors could also facilitate the overcoming of the disjoining-pressure barrier(s). For example, oil droplets contained within a foam migrate driven by the flow of the outgoing water. The motion of such a droplet could disturb the uniformity of the surfactant adsorption monolayers due to the hydrodynamic friction with the surfaces of the foam films or Plateau borders (Fig. 14.20a). The resulting nonuniform surfactant adsorption may have a destabilizing effect on the asymmetric oil-water-air films and could promote drop entry; this effect has not yet been modeled theoretically.

The experiment shows that the presence of small *solid crystallites* at the oil-water interface (Fig. 14.20b) facilitates the entry of an oil drop at the air-water interface [4, 52, 103-106]. Aveyard et al. [15] carried out experiments with separate foam films and observed that oil lenses at the film surface act together with hydrophobic solid to rupture the films. Wasan et al. [23] studied the effect of hydrophobic silica particles on the stability of *asymmetric* oil–water–air film formed at the tip of a glass capillary of inner diameter 200 – 300 μm. They established the existence of a critical (threshold) concentration of the solid particles, below which their antifoaming effect strongly decreases.

(a) Non-equilibrium Film Surfaces **(b) Piercing Effect of Solid Particles**

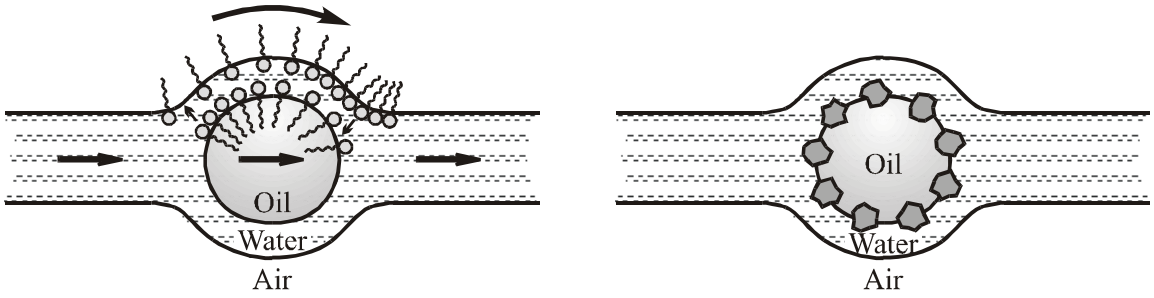

Fig. 14.20. Factors which promote overcoming of the disjoining-pressure barrier to oil-drop entry. (a) The motion of a migrating oil droplet, driven by the flow of the outgoing water, disturbs the uniformity of the surfactant adsorption monolayers due to the viscous friction. (b) Small solid crystallites, adsorbed at the oil-water interface, facilitate the rupturing of the asymmetric oil-water-air films.

Wang et al. [48] found out that hydrophobic silica particles concentrate in the oil-water interface. These authors observed that couples of oil lenses, attached to different surfaces of the Plateau border, merge upon contact to form a unstable oily bridge, whose rupture breaks the film/border. It seems that in this case the role of the solid particles is to rupture the *symmetric* oil-water-oil film between the two lenses and to effectuate the bridging.

Denkov et al. [18, 106] found out that the rupture of foam films by means of the bridging-stretching mechanism leads to a separation of the solid silica particles from the silicon oil droplets. Thus with the advance of the antifoaming process the initial, silica-containing oil drops, which exhibit a strong antifoaming action due to a synergistic effect, are transformed into two different populations of particles, silica-free and silica-enriched, both of them having a poor antifoaming performance. This is one of the possible mechanisms of antifoam deactivation (exhaustion) [18, 105, 106].

A powerful factor, which can bring about overcoming of the disjoining-pressure barrier, is the *evaporation* of water from the foam. It is known that a foam decays faster if it is exposed to atmosphere of lower humidity. The evaporation of water from the upper surface of a foam film is compensated by the influx of water from the neighboring Plateau border. The resulting viscous flow leads to a strong decrease of the local hydrodynamic pressure inside the film, which can cause overcoming of the barrier and film rupture. To estimate the latter effect let us consider a plane-parallel film, whose surfaces are circular disks of radius R. Equations (14.1) –

(14.4) are valid also in the present case. Water is supposed to evaporate only from the upper film surface (at $z = h$); then instead of Eq. (14.5) we have the following boundary condition:

$$v_z|_{z=0} = 0, \qquad v_z|_{z=h} = V_w j_e \tag{14.19}$$

Here j_e is the number of water molecules evaporating per unit time from unit area of the upper film surface; V_w is the volume per water molecule in the aqueous phase; h is the width of the gap in which the fluid flow takes place. The hydrodynamic pressure of the liquid in the film, P_l, is given by Eq. (14.8) with $u = -V_w j_e$:

$$P_l(r) = P_{PB} - \frac{3\eta V_w j_e}{h^3}(R^2 - r^2) \qquad (0 \le r \le R) \tag{14.20}$$

As before, r is the radial coordinate ($r = 0$ in the *center* of the film). The substitution of Eq. (14.20) into Eq. (14.16) yields

$$P_A = P_g - P_{PB} + \frac{2\sigma_{lg}}{R_f} + \frac{3\eta V_w j_e}{h^3}(R^2 - r^2) \tag{14.21}$$

The last term in Eq. (14.21) represents a viscous contribution to the capillary pressure difference applied across the film surface. The disjoining-pressure barrier (Fig. 14.17.a) will be overcome if $P_A > \Pi_{max}$; most probably this could happen in the center of the film (around $r = 0$), where the viscous contribution to P_A is maximal. With typical parameter values, $j_e \approx 6 \times 10^{17}$ cm^{-2} s^{-1} [107], $V_w = 30$ Å^2, $R = 0.1$ cm, $h = 100$ nm and $\eta = 0.01$ poises one obtains

$$3\eta V_w j_e R^2 / h^3 = 5.4 \times 10^5 \text{ Pa} \tag{14.22}$$

which is really a considerable effect. The same effect may strongly facilitate the entry of oil drops (captured in the foam) at the water-air interface. For the respective oil-water-air films both R and h are expected to be smaller than for the foam films. This would lead again to a large viscous contribution to P_A insofar as R^2 and h^3 enter, respectively, the numerator and denominator in Eq. (14.22) and the decreases in the values of these two parameters tend to compensate each other. In conclusion, the evaporation of water from the foam leads to a strong increase in the applied capillary pressure P_A due to viscous effects, which may cause overcoming of the disjoining pressure barrier(s) and possible film rupture.

The physical picture can be quite different if the surfactant solution contains *micelles* of low surface electric charge. In this case the evaporation-driven influx of water brings surfactant micelles in the foam film, just as it is depicted in Fig. 13.33, and, moreover, the electrostatic repulsion is not strong enough to expel the newcomers from the film. The water evaporates, but the micelles remain in the film; this leads to an increase of the micelle local concentration, and could even cause formation of surfactant *liquid crystal structures* within the film. This has been observed with mixed solutions of anionic surfactant with amphoteric one (betaine) [108]. The accumulation of surfactant within foam films has a stabilizing effect and can protect the films from rupturing.

14.4. SUMMARY AND CONCLUSIONS

Foams are produced in many processes in industry and every-day life. In some cases the foaminess is desirable, while in other cases it is not wanted. The fact that oil droplets, solid particles and their combination exhibit antifoaming action can be used as a tool for control of foam stability. In this aspect the knowledge about the mechanism of antifoaming action could be very helpful. The antifoaming action can be investigated in experiments with single films in the cells of Scheludko (Fig. 14.2) and Dippenaar (Fig. 14.14), as well as with vertical films formed in a frame (Figs. 14.3 and 14.13).

Direct observations show that when the foam decay is *slow* (from minutes to hours, see Fig. 14.6), the antifoam particles are expelled from the foam films into the Plateau borders. The breakage of foam cells happens when the surfaces of the thinning Plateau borders press the captured particles. The low rate of thinning of the Plateau borders is the reason for the low rate of foam decay in this case. In contrast, when the particles exhibit a *fast* antifoaming action, they are observed to break directly the foam films, which thin much faster than the Plateau borders; see Figs. 14.8 and 14.16. This leads to a greater rate of foam decay.

Three different mechanisms of antifoaming action have been established: *spreading* mechanism, *bridging-dewetting* and *bridging-stretching* mechanism, see Fig. 14.9. All of them involve as a necessary step the entering of an antifoam particle at the air-water interface, which is equivalent to rupture of the asymmetric particle-water-air film. Criteria for the entering, spreading and bridging to happen spontaneously have been proposed in terms of the respective

entering, spreading and bridging coefficients, see Eqs. (14.9) – (14.11). The experiment shows that the key determinant for antifoaming action is the stability of the asymmetric particle-water-air film, see the discussion concerning Table 14.1. Repulsive interactions in this film may create a high barrier to drop entry. The major *thermodynamic* factors, which stabilize the asymmetric film, are related to the presence of (i) barrier due to the *electrostatic* (double layer) repulsion, (ii) multiple barriers due to the *oscillatory structural forces* in micellar surfactant solution, (iii) barrier created by the *steric polymer-chain repulsion* in the presence of adsorbed nonionic surfactants. In addition, there are *kinetic* stabilizing factors, which damp the instabilities in the liquid films; such are (i) the *surface (Gibbs) elasticity*, (ii) the *surface viscosity* of the adsorption monolayers, (iii) the *adsorption relaxation time* related to the diffusion supply of surfactant from the bulk of solution.

On the other hand, a *foam-destabilizing* factor can be any attractive force operative in the liquid films, as well as any factor suppressing the effect of the aforementioned stabilizing factors. For example, the addition of salt reduces the height of the electrostatic and oscillatory-structural barriers in the case of *ionic* surfactant. Oscillatory-structural barriers due to nonionic-surfactant micelles are suppressed by the rise of temperature [69]. Solid particulates of irregular shape, adsorbed at the oil-water interface, have a "piercing effect" on asymmetric oil-water-air films and on symmetric oil-water-oil films as well.

It is worthwhile noting that some factors may have stabilizing or destabilizing effect depending on the specific conditions. For example, at low concentration the surfactant micelles have destabilizing effect because they give rise to the depletion attraction; on the other hand, at high concentration they exhibit stabilizing effect owing to the barriers of the oscillatory structural force. Likewise, oil droplets located in the Plateau borders of a foam have a foam-breaking effect when they are large enough (larger than 10 – 20 μm); on the other hand, smaller oil drops may block the outflow of water along the Plateau channels thus producing a foam-stabilizing effect. A third example is the effect of water evaporation from a foam: in the absence of surfactant micelles the evaporation-driven flux of water within the foam film creates strong viscous pressure, which helps to overcome the disjoining-pressure barrier(s), see Eq. (14.21); on the other hand, if micelles are present in the solution, the evaporation may increase their

concentration within the foam film and can create a stabilizing surfactant-structural barrier to film rupture.

The variety of factors and mechanisms may leave the discouraging impression that it is virtually impossible to predict and control the stability of foams and the antifoaming action of colloid particles. Accepting an optimistic viewpoint, we believe that it is still possible to give definite prescriptions and predictions based on the accumulated knowledge about the mechanisms of foam destruction. In this aspect, the role of an expert in foam stability resembles that of a medical doctor, who establishes the diagnosis and formulates prescriptions after a careful examination of each specific case.

14.5. REFERENCES

1. W. Gerhartz (Ed.), Ullmann's Encyclopedia of Industrial Chemistry, 5th ed., VCH Publishers, New York, 1988, pp. 466-490.
2. N.P. Ghildyal, B.K. Lonsane, N.G. Karanth, Adv. Appl. Microbiol. 33 (1988) 173.
3. J.I. Kroshwitz, M. Howe-Grant (Eds.), Kirk-Othmer Encyclopedia of Chemical Technology, Vol. 7, Wiley-Interscience, New York, 1993, pp. 430-447.
4. P.R. Garrett (Ed.), Defoaming: Theory and Industrial Applications, Marcel Dekker, New York, 1993.
5. R.D. Kulkarni, E.D. Goddard, P. Chandar, in: R.K. Prud'homme & S.A. Khan (Eds.) Foams: Theory, Measurements and Applications, Marcel Dekker, New York, 1995, p. 555.
6. D.T. Wasan, S.P. Christiano, in: K.S. Birdi (Ed.) Handbook of Surface and Colloid Chemistry, CRC Press, New York, 1997, pp. 179-215.
7. T.G. Rubel, Antifoaming and Defoaming Agents, Noyes Data Corp., Park Ridge, NJ, 1972.
8. H.T. Kerner, Foam Control Agents, Noyes Data Corp., Park Ridge, NJ, 1976.
9. J.C. Colbert, Foam and Emulsion Control Agents and Processes, Recent Developments, Noyes Data Corp., Park Ridge, NJ, 1981.
10. R. Aveyard, B.P. Binks, P.D.I. Fletcher, C.E. Rutherford, J. Dispersion Sci. Technol. 15 (1994) 251.
11. R.E. Patterson, Colloids Surf. A, 74 (1993) 115.
12. R.D. Kulkarni, E.D. Goddard, B. Kanner, Ind. Eng. Chem. Fund. 16 (1977) 472.
13. M.A. Ott, Modern Paints Coatings 67 (1977) 31.

14. I. Lichtman, T. Gammon, in: M. Grayson (Ed.), Kirk-Othmer Encyclopedia of Science and Technology, Vol. 7, Wiley-Interscience, New York, 1980, pp. 430-448.

15. R. Aveyard, P. Cooper, P.D.I. Fletcher, C.E. Rutherford, Langmuir 9 (1993) 604.

16. R. Aveyard, B.P. Binks, P.D.I. Fletcher, T.G. Peck, C.E. Rutherford, Adv. Colloid Interface Sci. 48 (1994) 93.

17. E.S. Basheva, D. Ganchev, N.D. Denkov, K. Kasuga, N. Satoh, K. Tsujii, Langmuir, 16 (2000) 1000.

18. N.D. Denkov, P. Cooper, J.-Y. Martin, Langmuir, 15 (1999) 8514.

19. R. Koczo, B. Ludanyi, Gy. Racz, Period. Polytech. Chem. Eng. 31 (1987) 83.

20. R.K. Prud'homme & S.A. Khan (Eds.) Foams: Theory, Measurements and Applications, Marcel Dekker, New York, 1995.

21. D. Exerowa, P.M. Kruglyakov, Foam and Foam Films, Elsevier, Amsterdam, 1998.

22. I.B. Ivanov, B.P. Radoev, T.T. Traykov, D.S. Dimitrov, E.D. Manev, C.S. Vassilieff, in E. Wolfram (Ed.) Proceedings of the International Conference on Colloid and Surface Science, Akademia Kiado, Budapest, 1975; p. 473.

23. D.T. Wasan, K. Koczo, A.D. Nikolov, Foams: Fundamentals and Application in the Petroleum Industry, in: L.L. Schram (Ed.) ACS Symp. Ser. No. 242, American Chemical Society, Washington D.C., 1994.

24. A. Scheludko, D. Exerowa, Kolloid–Z. 165 (1959) 148.

25. A. Scheludko, Adv. Colloid Interface Sci. 1 (1967) 391.

26. J. Mysels, J. Phys. Chem. 68 (1964) 3441.

27. M. Born, E. Wolf, Principles of Optics, 4th Ed., Pergamon Press, Oxford, 1970.

28. A. Vasicek, Optics of Thin Films, North Holland Publishing Co., Amsterdam, 1960.

29. A. Scheludko, Kolloid-Z. 155 (1957) 39.

30. E.S. Basheva, K.D. Danov, P.A. Kralchevsky, Langmuir 13 (1997) 4342.

31. K. Koczo, G. Racz, Colloids Surfaces 22 (1987) 97.

32. M.P. Aronson, Langmuir 2 (1986) 653.

33. K. Koczo, J.K. Koczone, D.T. Wasan, J. Colloid Interface Sci. 166 (1994) 225.

34. I.B. Ivanov, D.S. Dimitrov, Thin Film Drainage, in I.B. Ivanov (Ed.) Thin Liquid Films, Marcel Dekker, New York, 1988.

35. N.D. Denkov, Langmuir 15 (1999) 8530.

36. I.B. Ivanov, Pure Appl. Chem. 52 (1980) 1241.

37. O. Reynolds, Phil. Trans. Roy. Soc. (London) A177 (1886) 157.
38. L. D. Landau, E. M. Lifshitz, Fluid Mechanics, Pergamon Press, Oxford, 1984.
39. S. Ross, J.W. McBain, Ind. Eng. Chem. 36 (1944) 570.
40. S. Ross, J. Phys. Colloid Chem. 59 (1950) 429.
41. R.E. Pattle, J. Soc. Chem. Ind. 69 (1950) 363.
42. W.E. Ewers, K.L. Sutherland, Aust. J. Sci. Res. 5 (1952) 697.
43. L.T. Shearer, W.W. Akers, J. Phys. Chem. 62 (1958) 1264, 1269.
44. P.R. Garrett, J. Colloid Interface Sci. 69 (1979) 107.
45. P.R. Garrett, J. Colloid Interface Sci. 76 (1980) 587.
46. A. Dippenaar, Int. J. Mineral Process. 9 (1982) 1.
47. G.C. Frye, J.C. Berg, J. Colloid Interf. Sci. 127 (1989) 222; ibid. 130 (1989) 54.
48. G. Wang, R. Pelton, A. Hrymak, N. Shawafaty, Y.M. Heng, Langmuir 15 (1999) 2202.
49. J.V. Robinson, W.W. Woods, J. Soc. Chem. Ind. 67 (1948) 361.
50. W.D. Harkins, J. Chem. Phys. 9 (1941) 552.
51. A.W. Adamson, A.P. Gast, Physical Chemistry of Surfaces, 6th Ed., Wiley-Interscience, New York, 1997.
52. V. Bergeron, P. Cooper, C. Fischer, J. Giermanska-Kahn, D. Langevin, A. Pouchelon, Colloids Surf. A, 122 (1997) 103.
53. S. Ross, G. Young, Ind. Eng. Chem. 43 (1951) 2520.
54. S. Ross, A.F. Highes, M.L. Kennedy, A.R. Mardonian, J. Phys. Chem. 57 (1953) 684.
55. S. Ross, Chem. Eng. Progr. 63 (1967) 41.
56. P.M. Kruglyakov, T.T. Kotova, Doklady Akad. Nauk SSSR 188 (1969) 865.
57. R.S. Bhute, J. Sci. Ind. Res. 30 (1971) 241.
58. J.V. Povich, Am. Inst. Chem. Eng. J. 25 (1975) 1016.
59. S. Ross, G.M. Nishioka, J. Colloid Interface Sci. 65 (1978) 216.
60. R.M. Hill, S.P. Christiano, Antifoaming Agents, in J.C. Salamone (Ed.) The Polymeric Materials Encyclopedia, CRC Press, Boca Raton FL, 1996.
61. B.V. Derjaguin, Theory of Stability of Colloids and Thin Liquid Films, Plenum Press: Consultants Bureau, New York, 1989.
62. I.B. Ivanov, P.A. Kralchevsky, Mechanics and Thermodynamics of Curved Thin Liquid Films, in: I.B.Ivanov (Ed.) Thin Liquid Films, M. Dekker, New York, 1988, p. 49.

63. J.N. Israelachvili, Intermolecular & Surface Forces, Academic Press, London, 1992.

64. J.A. de Feijter, A. Vrij, J. Colloid Interface Sci. 70 (1979) 456.

65. A.D. Nikolov, D.T. Wasan, P.A. Kralchevsky, I.B. Ivanov, in: N. Ise and I. Sogami (Eds.), Ordering and Organisation in Ionic Solutions, World Scientific, Singapore, 1988.

66. A.D. Nikolov, D.T. Wasan, J. Colloid Interface Sci. 133 (1989) 1.

67. A. D. Nikolov, P. A. Kralchevsky, I. B. Ivanov, D. T. Wasan, J. Colloid Interface Sci. 133 (1989) 13.

68. P.A. Kralchevsky, A.D. Nikolov, D.T. Wasan, I. B. Ivanov, Langmuir 6 (1990) 1180.

69. A.D. Nikolov, D.T. Wasan, N.D. Denkov, P.A. Kralchevsky, I.B. Ivanov, Prog. Colloid Polym. Sci. 82 (1990) 87.

70. D.T. Wasan, A.D. Nikolov, P.A. Kralchevsky, I.B. Ivanov, Colloids Surf. 67 (1992) 139.

71. V. Bergeron, C.J. Radke, Langmuir 8 (1992) 3020.

72. M.L. Pollard, C.J. Radke, J. Chem. Phys. 101 (1994) 6979.

73. X.L. Chu, A.D. Nikolov, D.T. Wasan, Langmuir 10 (1994) 4403.

74. X.L. Chu, A.D. Nikolov, D.T. Wasan, J. Chem. Phys. 103 (1995) 6653.

75. P.A. Kralchevsky, N.D. Denkov, Chem. Phys. Lett. 240 (1995) 385.

76. K.G. Marinova, T.D. Gurkov, T.D. Dimitrova, R.G. Alargova, D. Smith, Langmuir 14 (1998) 2011.

77. I.B. Ivanov, P.A. Kralchevsky, Colloids Surfaces A, 128 (1997) 155.

78. K.D. Danov, P.A. Kralchevsky, I.B. Ivanov, Equilibrium and Dynamics of Surfactant Adsorption Monolayers and Thin Liquid Films, in: U. Zoller and G. Broze (Eds.) Handbook of Detergents, Vol. 1: Properties, Chapter 9; M. Dekker, New York, 1999.

79. A.J. Vries, Rec. Trav. Chim. Pays-Bas 77 (1958) 44.

80. A. Scheludko, Proc. K. Akad. Wetensch. B, 65 (1962) 87.

81. A. Vrij, Disc. Faraday Soc. 42 (1966) 23.

82. I.B. Ivanov, B. Radoev, E. Manev, A. Scheludko, Trans. Faraday Soc. 66 (1970) 1262.

83. I.B. Ivanov, D.S. Dimitrov, Colloid Polymer Sci. 252 (1974) 982.

84. P.A. Kralchevsky, K.D. Danov, I.B. Ivanov, Thin Liquid Film Physics, in: R.K. Prud'homme and S.A. Khan (Eds.) Foams, M. Dekker, New York, 1995, p.1.

85. I.B. Ivanov, K.D. Danov, P.A. Kralchevsky, Colloids and Surfaces A, 152 (1999) 161.

86. B.V. Derjaguin, Y.V. Gutop, Kolloidn. Zh. 24 (1962) 431.

87. B.V. Derjaguin, A.V. Prokhorov, J. Colloid Interface Sci. 81 (1981) 108.

88. A.V. Prokhorov, B.V. Derjaguin, J. Colloid Interface Sci. 125 (1988) 111.

89. D. Kashchiev, D. Exerowa, J. Colloid Interface Sci. 77 (1980) 501.

90. D. Kashchiev, D. Exerowa, Biochim. Biophys. Acta 732 (1983) 133.

91. D. Kashchiev, Colloid Polymer Sci. 265 (1987) 436.

92. Y.A. Chizmadzhev, V.F. Pastushenko, Electrical Breakdown of Bilayer Lipid Membranes, in: I.B. Ivanov (Ed.) Thin Liquid Films, M. Dekker, New York, 1988; p. 1059.

93. L.V. Chernomordik, M.M. Kozlov, G.B. Melikyan, I.G. Abidor, V.S. Markin, Y.A. Chizmadzhev, Biochim. Biophys. Acta 812 (1985) 643.

94. L.V. Chernomordik, G.B. Melikyan, Y.A. Chizmadzhev, Biochim. Biophys. Acta 906 (1987) 309.

95. A. Kabalnov, H. Wennerström, Langmuir 12 (1996) 276.

96. I.B. Ivanov, S.K. Chakarova, B. I. Dimitrova, Colloids Surf. 22 (1987) 311.

97. B.I. Dimitrova, I.B. Ivanov, E. Nakache, J. Dispers. Sci. Technol. 9 (1988) 321.

98. K.D. Danov, I.B. Ivanov, Z. Zapryanov, E. Nakache, S. Raharimalala, in: M.G. Velarde (Ed.) Proceedings of the Conference of Synergetics, Order and Chaos, World Scientific, Singapore, 1988, p. 178.

99. C.V. Sterling, L.E. Scriven, AIChE J. 5 (1959) 514.

100. S.P. Lin, H.J. Brenner, J. Colloid Interface Sci. 85 (1982) 59.

101. J.L. Castillo, M.G. Velarde, J. Colloid Interface Sci. 108 (1985) 264.

102. D.S. Valkovska, P.A. Kralchevsky, K.D. Danov, G. Broze, A. Mehreteab, Langmuir 16 (2000) 8892.

103. J.K. Angarska, K.D. Tachev, P.A. Kralchevsky, A. Mehreteab, B. Broze, J. Colloid Interface Sci. 200 (1998) 31.

104. P.R. Garrett, J. Davis, H.M. Rendall, Colloids Surf. A, 85 (1994) 159.

105. A. Pouchelon, A. Araud, J. Dispersion Sci. Technol. 14 (1993) 447.

106. N.D. Denkov, K.G. Marinova, C. Christova, A. Hadjiiski, P. Cooper, Langmuir 16 (2000) 2515.

107. C.D. Dushkin, H. Yoshimura, K. Nagayama, Chem. Phys. Lett. 204 (1993) 455.

108. D. Ganchev, E. Ahmed, N. Denkov, Fac. Chem., Univ. Sofia, private communication.